Metallocene Antitumor Agents. Solution and Solid-State Molybdenocene Coordination Chemistry of DNA Constituents

Louis Y. Kuo,† Mercouri G. Kanatzidis, Michal Sabat, Andrew L. Tipton, and Tobin J. Marks*

Contribution from the Department of Chemistry, Northwestern University, Evanston, Illinois 60208. *Received April 25, 1991*

Abstract: This contribution reports a solution and solid-state structural study of the aqueous nucleobase and nucleotide coordination chemistry of the organometallic antineoplastic agent, Cp_2MoCl_2 (**1**, Cp = η^5-C_5H_5). In neutral aqueous solution, Cp_2MoCl_2 undergoes essentially complete chloride aquation within 60 min to yield what is formulated as $Cp_2Mo(H_2O)OH^+$, while under the same conditions, the Mo–Cp bonds are hydrolytically stable. Reaction of aqueous Cp_2MoCl_2 with the alkylated nucleobases, 9-methyladenine and 1-methylcytosine yields two isomeric [Cp_2Mo(9-methyladenyl)][PF_6] complexes (**3a** and **3b**) and a single isomer of [Cp_2Mo(1-methylcytosyl)][PF_6] (**4**). On the basis of solution NMR spectroscopy, **3a** and **3b** are assigned HN6$^-$/N1 and HN6$^-$/N7 chelation modes, respectively, while **4** involves an HN4$^-$/N3 chelation mode. Complex **3a** crystallizes in the triclinic space group $P\bar{1}$ with a = 10.682 (3) Å, b = 11.619 (5) Å, c = 7.701 (5) Å, α = 106.93 (4)°, β = 96.32 (3)°, γ = 86.98 (3)°, V = 908.64 Å^3, Z = 2; $R(F)$ = 0.045 for 3614 independent reflections having $I > 3\sigma(I)$. The Cp_2Mo^{2+} fragment is in a bent sandwich geometry with an average Mo–C distance of 2.309 (4) Å, a Mo–N1 distance of 2.173 (3) Å, a Mo–N6 distance of 2.145 (3) Å, a N1–Mo–N6 angle of 60.9 (1)°, and a ring centroid–Mo–ring centroid angle of 135.3°. The 9-methyladenyl ligand in **3a** lies in the plane which bisects the ring centroid–Mo–ring centroid angle. Chelation constricts the N6–C6–N1 angle to 108.5 (3)°. Complex **4** crystallizes in the monoclinic space group ($P2_1/c$) with a = 11.703 (1) Å, b = 10.794 (2) Å, c = 14.416 (2) Å, β = 111.28 (1)°, Z = 4, V = 1696.8 Å^3; $R(F)$ = 0.047 for 3007 independent reflections having $I > 3\sigma(I)$. The Cp_2Mo^{2+} fragment is also in a bent sandwich geometry with an average Mo–C distance of 2.294 (7) Å, a Mo–N4 distance of 2.140 (5) Å, a Mo–N3 distance of 2.130 (5) Å, a N1–Mo–N6 angle of 59.9 (1)°, and a ring centroid–Mo–ring centroid angle of 136.5°. The 1-methylcytosyl ligand in **4** lies in the plane which bisects the ring centroid–Mo–ring centroid angle, and chelation constricts the N4–C4–N3 angle to 106.8 (5)°. On the NMR time scale and in the absence of other competing ligands, complex **1** forms 1:1 complexes with the 2′-deoxyribonucleotide-5′-monophosphates of guanosine (5′-dGMP), adenosine (5′-dAMP), cytosine (5′-dCMP), and thymidine (5′-dTMP). There is little selectivity in the complexation, and nucleotide–nucleotide exchange processes are detectable. Although nucleotide complexation is observed, there is no NMR evidence that Cp_2MoCl_2(aq) disrupts Watson–Crick base pairing in 5′-dGMP/5′-dCMP or 5′-dAMP/5′-dTMP dimers. The Cp_2Mo^{2+} adduct of 5′-dGMP (**5**) crystallizes in the triclinic space group $P\bar{1}$ with a = 10.690 (3) Å, b = 14.567 (5) Å, c = 9.298 (3) Å, α = 107.20 (2)°, β = 99.22 (3)°, γ = 77.62 (3)°, Z = 1, V = 1344 (2) Å^3; $R(F)$ = 0.045 for 5491 independent reflections having $I > 3\sigma(I)$. The crystal structure of complex **5** consists of dimeric [Cp_2Mo(5′-dGMP)]$_2$ units interconnected by water bridges. Each Cp_2Mo^{2+} unit of the dimer is in a bent sandwich geometry and is coordinated to N7 and O(phosphate) of different 5′-dGMP moieties. Metrical parameters for **5** are as follows: Mo–C distance(av), 2.307 (9) Å; Mo–N7 distance, 2.20 (1) Å; Mo–O(phosphate) distance, 2.096 (9) Å; N7–Mo–O(phosphate) angle, 77.8 (2)°; and ring centroid–Mo–ring centroid angle, 133.8 (6)°. The 5′-dGMP unit has β^{gg} and γ^{gt} torsional conformers and exhibits an unusual syn glycosidic and C3′-endo sugar puckering conformation. Compound **1** forms a monomeric complex with 5′-dAMP (**6**) in aqueous solution via Mo–N7 and Mo–O(phosphate) chelation, two complexes with 5′-dCMP that both involve O(phosphate) coordination, and a single complex with 5′-dTMP which involves O(phosphate) and N3 coordination. These results place significant ligational restrictions on the mode(s) by which Cp_2MX_2(aq) species might bind to DNA and, together with a molecular graphics investigation of Cp_2Mo^{+2} coordination to a model oligonucleotide duplex, argue against cisplatinlike complexation motifs.

Introduction

Köpf and Köpf-Maier have shown that the metallocene dihalides Cp_2MX_2, A (Cp = η^5-C_5H_5; M = Ti, V, Nb, Mo; X = F, Cl, Br, I, NCS, and N_3) are highly active agents against a variety of tumor cell lines including Ehrlich ascites, B16 melanoma, colon 38

A

carcinoma, Lewis lung carcinoma, lymphoid leukemia L1210, lymphocytic leukemia P388 as well as several human colon and lung carcinomas heterotransplanted in athymic mice.[1-3] In parallel studies, we have shown that Cp_2VCl_2 is as active as *cis*-dichlorodiammineplatinum ("cisplatin")[4] against human epidermoid (HEP-2) tumor cells in vitro and against mouse mammary tumor cells (TA3Ha) in vivo.[5,6] Thus, the Cp_2MX_2 complexes constitute a potent new class of organometallic antitumor agents.

Like cisplatin,[4,7] the metallocene dichlorides have also been shown to inhibit DNA biosynthesis[8] and mitotic activity in cancer

† Present address: Department of Chemistry, Lewis and Clark College, Portland, OR 97219.

(1) (a) Köpf-Maier, P.; Köpf, H. *Struct. Bond.* **1988**, *70*, 105–185, and references therein. (b) Köpf-Maier, P.; Köpf, H. *Drugs of the Future* **1986**, *11*, 297–319, and references therein.

(2) (a) Köpf-Maier, P.; Moormann, A.; Köpf, H. *Eur. J. Cancer Clin. Oncol.* **1985**, *21*, 853–857. (b) Köpf-Maier, P.; Wagner, W.; Köpf, H. *Cancer Chemother. Pharmacol.* **1981**, *5*, 237–241. (c) Köpf-Maier, P.; Wagner, W.; Hesse, B.; Köpf, H. *Eur. J. Cancer* **1981**, *17*(6), 665–669. (d) Köpf-Maier, P.; Hesse, B.; Voigtlander, R.; Köpf, H. *J. Cancer Res. Clin. Oncol.* **1980**, *97*, 31–39. (e) Köpf-Maier, P.; Hesse, B.; Köpf, H. *J. Cancer Res. Clin. Oncol.* **1980**, *96*, 43–51. (f) Köpf-Maier, P.; Leitner, M.; Köpf, H. *J. Inorg. Nucl. Chem.* **1980**, *42*, 1789–1791. (g) Köpf-Maier, P.; Leitner, M.; Voigtlander, R.; Köpf, H. *Z. Naturforsch B.: Anorg. Chem. Org. Chem.* **1979**, *34C*, 1174–1176. (h) Köpf-Maier, P.; Köpf, H. *Z. Naturforsch. B.: Anorg. Chem. Org. Chem.* **1979**, *34B*, 805–807. (i) Köpf, H.; Köpf-Maier, P. *Angew. Chem., Int. Ed. Engl.* **1979**, *18*, 477–478.

(3) There is now evidence that free cyclopentadiene is not the active agent: (a) Köpf-Maier, P.; Köpf, H. *J. Organomet. Chem.* **1988**, *342*, 167–176. (b) Murthy, M. S.; Rao, L. N.; Kuo, L. Y.; Marks, T. J., manuscript in preparation. Globally administered CpH cytotoxity against human HEp-2 carcinoma is only apparent when the administered concentration is 10^3× greater than the corresponding therapeutic concentration of Cp_2VCl_2.

(4) (a) Rosenberg, B. *Cancer* **1985**, *55*, 2303–2316. (b) *Platinum Coordination Complexes in Chemotherapy*; Hacker, M. P., Douple, E. B., Krakoff, I. H., Eds.; Nijhoff Publishers: Boston, MA, 1984. (c) *Platinum, Gold, and Other Metal Chemotherapeutic Agents*; *ACS Symp. Ser.* **1983**, *209*. (d) Einhorn, L. H. *Cancer Res.* **1981**, *41*, 3275–3280.

0002-7863/91/1513-9027$02.50/0

Scheme I

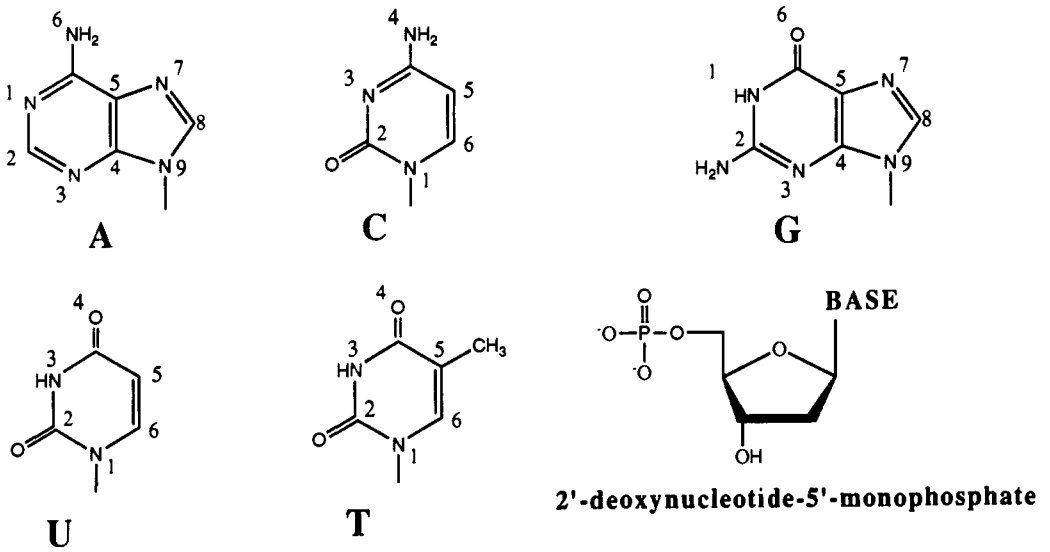

cells.[9] It has also been demonstrated that the respective metals of Cp_2VCl_2 and Cp_2TiCl_2 accumulate in the nucleic acid-rich regions of tumor cells.[10] These biological congruencies between the metallocene dichlorides and cisplatin along with the obvious structural similarity of *cis*-MX_2 functionality[11] have led to the speculation[1] that the mechanistic activity of the metallocene drugs involves DNA as the primary biological target, perhaps in a coordinative manner similar to cisplatin.

A goal of our research has been to elucidate the aqueous coordination chemistry of the metallocene drugs with DNA models of varying complexity. The results should be valuable in understanding the mechanism of carcinostatic activity as well as in laying the foundations for the rational design of more active organometallic antineoplastic agents. We have previously shown that strong chemical *dissimilarities* exist between cisplatin and the groups 4,5 metallocene dichlorides. Under physiological conditions, these Cp_2MCl_2 complexes (M = Ti, Zr, and V) undergo far more rapid and extensive chloride hydrolysis than does cisplatin.[12] In addition, the Ti–C_5H_5 and Zr–C_5H_5 ligation is hydrolytically unstable.[12] In contrast to cisplatin,[7] we have shown that the binding of Cp_2VCl_2(aq) to nucleotides is labile on the NMR time scale and predominantly phosphate-centered, with minimal disruption of Watson–Crick base pairing.[13] These marked differences raise many molecular-scale questions concerning the interaction of the metallocene dichlorides with DNA and any parallels to cisplatin–DNA coordination chemistry.

In the present contribution, we extend these studies to a "softer" group 6 system and report a chemical/physicochemical investigation of the coordination chemistry of aqueous molybdenocene dichloride with DNA constituents.[14] The goals were to investigate the aqueous solution chemistry of Cp_2MoCl_2 and to establish the nature of Mo(IV) coordination to DNA building blocks including representative 2′-deoxynucleotide-5′-monophosphates (Scheme I) and alkylated nucleobases under physiological conditions (mM concentration in Cp_2MoCl_2 and pH = 7.2–7.4). This coordination chemistry can be readily elucidated using FT NMR techniques. It will be seen that the Mo–Cp ligation is hydrolytically stable while chloride hydrolysis is complete and extremely rapid and that the coordination of aqueous Cp_2MoCl_2 to DNA constituents is radically different from that of Cp_2VCl_2. On the NMR time scale and in the absence of other competing ligands, Cp_2MoCl_2(aq) coordinates to *both* the nucleobase (N) and phosphate (O) moieties of mononucleotides in a relatively nonlabile manner that effects major conformational changes within the mononucleotide. In addition, we present the crystal structures of the model compounds, [Cp_2Mo(9-methyladenyl)][PF_6] (**3a**), [Cp_2Mo(1-methylcytosyl)][PF_6] (**4**), and [Cp_2Mo(2′-deoxyguanosine-5′-monophosphate)]$_2$ (**5**), which confirm the spectroscopically derived solution coordination patterns and provide important metrical details. These results and their implications for Cp_2Mo^{2+} binding to DNA vis-ā-vis that of cisplatin are also discussed.

Experimental Section

All organometallic compounds were handled under prepurified nitrogen using standard Schlenk or glovebox techniques. Organic solvents were deoxygenated with three freeze–pump–thaw cycles, and water was deionized, distilled, and thoroughly purged with prepurified nitrogen. The complex Cp_2MoCl_2 (**1**) (Strem Chemical Co., Newburyport, MA) was used as received. Purity was checked by ^{1}H NMR and IR spectroscopy and by elemental analysis. Me_2SO-d_6 was dried by refluxing over BaO overnight, vacuum transferred onto freshly activated molecular sieves (4Å), and deoxygenated with three freeze–pump–thaw cycles. D_2O as well as all NaOH and HCl solutions were thoroughly saturated with N_2. 2′-Deoxynucleotide-5′-monophosphates (disodium salts and free acids) were obtained from Sigma Chemical Co. (St. Louis, MO) and purified by precipitation from an aqueous solution with acetone. Purity was verified with ^{1}H and ^{31}P NMR spectroscopy. 1-Methylcytosine was also obtained from Sigma Chemical Co. and used as received. 9-Methyladenine was synthesized and purified according to the procedure of Myers and Zelenznick.[15] All other chemicals were reagent grade and

(5) (a) Murthy, M. S.; Toney, J. H.; Rao, L. N.; Kuo, L. Y.; Marks, T. J. *Proc. Am. Assoc. Cancer Res.* **1986**, *27*, 279. (b) Toney, J. H.; Rao, L. N.; Murthy, M. S.; Marks, T. J. *Breast Cancer Res. Treat.* **1985**, *6*, 185.

(6) Murthy, M. S.; Rao, L. N.; Kuo, L. Y.; Toney, J. H.; Marks, T. J. *Inorg. Chim. Acta* **1988**, *152*, 117–124.

(7) (a) Bruhn, S. L.; Toney, J. H.; Lippard, G. J. *Prog. Inorg. Chem.* **1990**, *38*, 477–516. (b) Lippert, B. *Prog. Inorg. Chem.* **1989**, *37*, 1–97. (c) Reedijk, J.; Fichtinger-Schepman, A. M. J.; van Oosterom; van do Putte, P. *Struct. Bond. (Berlin)* **1987**, *67*, 1153–1181. (d) Sherman, S. E.; Lippard, S. J. *Chem. Rev.* **1987**, *87*, 1153–1181. (e) Barnard, C. F. J.; Cleare, M. J.; Hydes, P. C. *Chem. Brit.* **1986**, *22*, 1001–1004. (f) *Biochemical Mechanisms of Platinum Antitumor Drugs*; McBrien, D. C. H., Slater, T. F., Eds.; IRL Press: Oxford, 1986. (g) Pinto, A.; Lippard, S. J. *Biochim. Biophys. Acta* **1985**, *780*, 167–180.

(8) (a) Köpf-Maier, P.; Wagner, W.; Köpf, H. *Naturwissenschaften* **1981**, *68*, 272–273. (b) Köpf-Maier, P.; Köpf, H. *Naturwissenschaften* **1980**, *67*, 415–416.

(9) Köpf, H.; Köpf-Maier, P. in ref 4c, pp 315–333.

(10) (a) Köpf-Maier, P.; Krahl, D. *Chem.-Biol. Interact.* **1983**, *44*, 317–328. (b) Köpf-Maier, P.; Köpf, H. *Naturwissenschaften* **1981**, *68*, 273–274.

(11) Cl–M–Cl angle: $(H_3N)_2PtCl_2$, 91.9 (3)°; $(C_5H_4CH_3)_2VCl_2$, 87.06 (9)°; Cp_2TiCl_2, 94.43 (6)°; Cp_2MoCl_2, 82.0 (2)°; Cp_2ZrCl_2, 97.1°. See: ref 1b, p 317.

(12) Toney, J. H.; Marks, T. J. *J. Am. Chem. Soc.* **1985**, *107*, 947–953.

(13) Toney, J. H.; Brock, C. P.; Marks, T. J. *J. Am. Chem. Soc.* **1986**, *108*, 7263–7274.

(14) Preliminary communications: (a) Kuo, L. Y.; Sabat, M.; Tipton, A. L.; Marks, T. J. Third Chemical Congress of North America, Toronto, June 1988; Abstract 410. (b) Kuo, L. Y.; Kanatzidis, M. G.; Marks, T. J. *J. Am. Chem. Soc.* **1987**, *109*, 7207–7209.

(15) Myers, T. C.; Zeleznick, L. *J. Org. Chem.* **1963**, *28*, 2087–2089.

were obtained from Aldrich Chemical Co. (Milwaukee, WI) and used as received. The monomethylphosphate ester of 2'-deoxyguanosine-5'-monophosphate was synthesized as described by Marzilli,[16] and the purity was verified by ^1H and ^{31}P NMR spectroscopy.

Physical and Analytical Measurements. Proton and phosphorus NMR spectra were recorded on a JEOL FX-270 (FT, 270 and 109 MHz) or a Varian XLA-400 (FT, 400 and 161 MHz) spectrometer. Integration studies were recorded with 5-s pulse delays, and proton–proton coupling constants were determined by selective decoupling experiments. Proton chemical shifts are referenced to Me_4Si (TMS) and phosphorus chemical shifts to methylenediphosphonic acid (18.5 ppm relative to external 85% H_3PO_4) contained in a coaxial insert. Infrared spectra were recorded on Perkin-Elmer 599 or 283 spectrometers. Sample mulls were prepared in a glovebox with dry, degassed Nujol and were studied between KBr plates in an air-tight, O-ring sealed holder. FAB/MS spectra were measured on a VG 70-250 SE instrument, and cryoscopic molecular weight measurements were carried out with a modified Knauer Type 24.00 cryoscopic unit. pH measurements were carried out with an American Scientific pH 1 meter and a Broadley-Jones pH electrode having an internal reference or with a Wilmad combination pH electrode. Unless otherwise noted, all reported pD values in D_2O are corrected pH readings (pD = pH + 0.44).[17] Elemental analyses were performed by Dornis and Kolbe Mikroanalytisches Laboratorium (Mulheim, W. Germany).

Equilibrium and kinetic measurements of the hydrolytic loss of chloride and cyclopentadienyl ligands from Cp_2MoCl_2 were performed as previously described[12] over a 10-fold concentration range in Cp_2MoCl_2 (4 mM–40 mM).

The high-resolution solid-state CPMAS ^{31}P NMR spectrum of $[Cp_2Mo(5'\text{-dGMP})]_2$ (**5**) was measured at 120.8 MHz on a Varian VXR-300 spectrometer equipped with a Doty Scientific 5 mm high spinning speed solids probe. Anaerobic sample handling techniques were employed, and boil-off nitrogen gas was used to spin the sample at 6 kHz. To achieve a satisfactory spectrum, 7406 transients were collected. The spectrum was referenced to liquid H_3PO_4 (85%) by the substitution method.

Nuclear Overhauser enhancement (NOE) experiments were performed in D_2O solutions maintained at 23.6 °C using the Varian XLA-400 spectrometer. A 15-s pulse delay was employed, and an interleaving data collection of 16 scans was used to compensate for possible spectrometer instabilities. Possible paramagnetic impurities in the D_2O were removed by passing through Chelex-100 (Sigma Chemical Co., St. Louis, MO). The $[Cp_2Mo(5'\text{-dGMP})]_2$ complex (**5**) was thoroughly washed with D_2O, and the $Cp_2Mo(5'\text{-dAMP})$ adduct (6) was precipitated from a D_2O solution with acetone. The Cp_2Mo–nucleotide complexes were then dissolved in D_2O (concentration range ca. 0.5–1.0 mM), and the solutions were purged with N_2 for 40 min prior to NOE measurements. The percentage NOE was measured as described by Derome.[18]

Synthesis of $(C_5H_5)_2Mo(OH)(H_2O)^+B(C_6H_5)^-_4\cdot{}^1/_2H_2O$ (2). The tetraphenylborate salt of aqueous Cp_2MoCl_2 was isolated by slow diffusion of a 120 mM (pH 7.4) aqueous $NaBPh_4$ solution into 5.0 mL of a 34 mM Cp_2MoCl_2 solution (pH 7.4) in a Schlenk tube. The pH adjustments were made with either concentrated NaOH or HCl. After seven days, light green, air-sensitive flakes were isolated from the mother liquor by filtration, washed with cold H_2O, and dried in vacuo: yield 77% (74 mg); ^1H NMR (Me_2SO-d_6) δ 7.14 (s, 8 H), 6.92 (t, 8 H), 6.78 (t, 4 H), 5.95 (s, 10 H); IR data (cm^{-1}) 3440 w, 3340 w, 3100 m, 3050 m, 1590 m, 1578 m, 1422 s, 1373 s, 1262 m, 1147 m, 1062 m, 1015 w, 1025 w, 995 w, 835 s, 735 vs, 702 vs, 602 s; FAB/MS m/e = 261. Anal. Calcd for $[(C_5H_5)_2Mo(OH)(H_2O)][B(C_6H_5)_4](H_2O)_{0.5}$:C, 69.16; H, 5.98; MW (for cationic portion only) = 260.[19] Found: C, 68.98; H, 5.79.

Synthesis of $[Cp_2Mo(9\text{-methyladenyl})][PF_6]$ (3a). A 100-mL Schlenk flask equipped with a magnetic stir bar was charged with 161 mg (1.08 mmol) of 9-methyladenine and 160 mg (0.539 mmol) Cp_2MoCl_2 in the glovebox. On the Schlenk line, 16 mL of H_2O was syringed into the flask under a nitrogen flush, and the mixture was stirred until dissolution was complete (~1 h). The pH of the green solution was then brought to 7.55 with concentrated NaOH(aq), resulting in a deep red solution that was then stirred at 39 °C for 16 h. After cooling the solution to room temperature, it was cannula-filtered and evaporated in vacuo. The red residue was redissolved in methanol, cannula-filtered again, and evaporated in vacuo, and the solvent was replaced with 30 mL of H_2O. The $[Cp_2Mo(9\text{-methyladenyl})]^+$ complex was then precipitated by addition of 2 mL of a NH_4PF_6 solution (500 mg), and the mixture was then stirred for 18 h at 90 °C to redissolve the red precipitate. Slow cooling of the filtered, pale red $[Cp_2Mo(9\text{-methyladenyl})][PF_6]$ solution in a Schlenk tube afforded thin red needles that were washed with cold H_2O and dried under vacuum: yield 20% (33.8 mg).

^1H NMR spectroscopy showed the thin red needles to be composed of both isomer **3a** (90%) and **3b** (10%). Isomer **3b** was obtained by heating **3a** at 80 °C in water for seven days followed by recrystallization from an acetone/ether solution. Isomer **3a** was recrystallized for X-ray analysis by slow vapor diffusion of ether into an acetone solution.[20a] ^1H NMR spectral assignment of the H2 and H8 resonances of the 9-methyladenine ligand was verified using 9-methyladenine deuterated at C8 according to the procedure of Charland and Beauchamp:[20b] ^1H NMR (Me_2SO-d_6) isomer **3a** δ 8.00 (s, 1 H), 7.64 (s, 1 H), 6.90 (s, 1 H), 5.84 (s, 10 H), 3.66 (s, 3 H); isomer **3b** 8.32 (s, 1 H), 8.16 (s, 1 H), 6.46 (s, 1 H), 5.88 (s, 1 H), 3.80 (s, 3 H); IR data (cm^{-1}) for **3a** 3150 s, 3057 s, 1610 s, 1548 m, 1520 w, 1418 s, 1405 s, 1325 s, 1292 m, 1240 s, 1202 m, 1127 m, 1057 s, 1026 s, 998 m, 948 m, 930 w, 825 s, 750 s, 728 m, 656 w, 636 m, 545 s, 525 w, 490 m; FAB/MS for **3b** m/e = 377. Anal. Calcd for $C_{16}H_{16}N_5MoPF_6$: C, 37.01; H, 3.11; N, 13.49; P, 5.97; MW = 376. Found for **3a**: C, 36.80; H, 3.00; N, 13.22; P, 5.94. Found for **3b**: C, 36.89; H, 3.07; N, 13.38; P, 5.89.

Synthesis of $[Cp_2Mo(1\text{-methylcytosyl})][PF_6]$ (4). In the glovebox, a 100-mL Schlenk flask equipped with a magnetic stir bar was charged with 104 mg (0.832 mmol) of 1-methylcytosine and 130 mg (0.438 mmol) of Cp_2MoCl_2. On the Schlenk line, 12 mL of H_2O was syringed into the flask under nitrogen flush, and the mixture was stirred until dissolution was complete (~1 h). The pH was then adjusted to 7.30 with aqueous NaOH solution, and the red reaction mixture was stirred for 17 h at 40 °C. After cooling the solution to room temperature, it was filtered through a Schlenk frit, the solvent was removed in vacuo, the residue was dissolved in 15 mL of methanol, and the solution was filtered via cannula. The methanol was then removed in vacuo and replaced with 15 mL of H_2O. The $[Cp_2Mo(1\text{-methylcytosyl})]^+$ cation was next precipitated by addition of 2 mL of an aqueous NH_4PF_6 solution (300 mg), and the mixture then was stirred for 18 h at 80–90 °C to redissolve the red precipitate. Slow cooling of the filtered red solution in a Schlenk tube afforded long thin red needles that were washed with cold water and dried in vacuum: yield 26% (40 mg). Crystals for X-ray diffraction studies were grown by vapor diffusion of ether into an acetone solution: ^1H NMR (Me_2SO-d_6) δ 7.53 (d, 1 H), 6.42 (s, 1 H), 5.74 (s, 10 H), 5.15 (d, 1 H), 3.17 (s, 3 H); ^{13}C NMR (Me_2SO-d_6) δ 182, 153, 148, 98.2, 94.0, 36.0; IR data (cm^{-1}) 3418 s, 3270 s, 3120 s, 1658 s, 1615 s, 1560 s, 1531 m, 1460 s, 1420 s, 1375 s, 1335 s, 1298 m, 1257 w, 1225 m, 1183 w, 1138 w, 1014 s, 961 m, 932 m, 840 s, 780 s, 763 s, 743 m, 735 m, 645 m, 550 s, 532 m, 474 m, 435 m. Anal. Calcd for $C_{15}H_{16}N_3MoPF_6$: C, 36.36; H, 3.23; N, 8.48; P, 6.26. Found: C, 36.38; H, 3.30; N, 8.38; P, 6.34.

Synthesis of $[Cp_2Mo(5'\text{-dGMP})]_2$ (5). A Schlenk tube was charged with 60 mg (0.17 mmol) of $Na_2(5'\text{-dGMP})$ and an equimolar amount of Cp_2MoCl_2 (51 mg) in the glovebox. On the Schlenk line, 2 mL of D_2O was syringed in, and the pD of the green solution was brought up to 7.4 with concentrated aqueous NaOD. The solution was then transferred to a 5-mm NMR tube, and after 24 h at 25 °C, aqua-green crystals were isolated by removing the mother liquor under a nitrogen flush and then washing them with cold D_2O: yield, 35% (68 mg); ^1H NMR (D_2O) δ 7.90 (s, 1 H), 5.69 (s, 5 H), 5.44 (s, 5 H), 6.05 (t, 1 H), 4.50 (m, 1 H), 3.94 (m, 1 H), 3.80 (m, 2 H), 2.71 (m, 1 H), 2.45 (m, 1 H); IR data (cm^{-1}) 3140 s, 1675 s, 1560 s, 1460 s, 1420 s, 1340 m, 1318 m, 1285 m, 1267 m, 1190 s, 1050 s, 955 s, 832 s, 775 s, 730 s, 709 m, 639 m, 587 m, 572 m, 552 m, 532 m, 513 m. FAB/MS for **5** m/e = 1144. Anal. Calcd for $C_{40}H_{44}O_{14}N_{10}Mo_2P_2$: C, 42.03; H, 3.85; N, 12.26; P, 5.43; MW = 1144. Found: C, 41.89; H, 4.23; N, 12.15; P, 5.42.

Synthesis of $Cp_2Mo(5'\text{-dAMP})$ (6). In the glovebox, a 100-mL Schlenk flask was charged with 180 mg (0.605 mmol) of Cp_2MoCl_2 and 200 mg (0.600 mmol) of the 5'-dAMP diacid. On the Schlenk line, 25 mL of H_2O was syringed into the flask under nitrogen flush, and the pH was brought to 7.5 with Et_3N. The red/green reaction mixture was then stirred for 5 h at 35 °C, and after cooling to room temperature, the water was evaporated in vacuo. The Et_3NHCl was removed by Soxhlet extraction with CH_2Cl_2 under reduced pressure at 40 °C for 18 h. After

(16) Miller, S. K.; VanDerveer, D. G.; Marzilli, L. G. *J. Am. Chem. Soc.* **1985**, *107*, 1048–1055.

(17) Glasoe, P. K.; Long, F. A. *J. Phys. Chem.* **1960**, *64*, 188–190.

(18) Derome, A. E. *Modern NMR Techniques for Chemistry Research*; Pergamon Press: England, 1987; pp 97–127.

(19) Other Cp_2Mo derivatives that can be eliminated on the basis of elemental analysis are $Cp_2Mo{=}O$ calcd C, 49.79; H, 4.14, and $[Cp_2Mo(OH_2)_2OMoCp_2][BPh_4]$ calcd C, 72.08; H, 5.65. Furthermore, in the FAB/MS of **2**, no molecular ion peaks are found in the region above m/e = 300 that could be associated with oligomeric forms of $Cp_2Mo(OH)(OH_2)^+$.

(20) (a) Crystals of isomer **3b** were also grown by diffusion of ether into an acetone solution. However, they were not of diffraction quality. (b) Charland, J.; Beauchamp, A. L. *Croat. Chem. Acta* **1984**, *57*, 693–701.

removal of the CH_2Cl_2 in vacuo, the green $Cp_2Mo(5'\text{-dAMP})$ complex was washed with methanol and dried under vacuum: yield 10% (33 mg); ^1H NMR ($Me_2SO\text{-}d_6$) δ 8.30 (s, 1 H), 8.13 (s, 1 H), 7.26 (s, 2 H), 6.38 (t, 1 H), 5.76 (s, 5 H), 5.71 (s, 5 H), 4.46 (m, 1 H), 3.95 (m, 1 H), 3.83 (m, 2 H), 2.34 (m, 1 H), 2.15 (m, 1 H); ^1H NMR (D_2O) δ 8.11 (s, 1 H), 7.97 (s, 1 H), 6.21 (t, 1 H), 5.68 (s, 5 H), 5.31 (s, 5 H), 4.50 (m, 1 H), 4.00 (m, 1 H), 3.81 (m, 2 H), 2.74 (m, 1 H), 2.57 (m, 1 H); ^{31}P NMR ($Me_2SO\text{-}d_6$) δ 42.0; ^{31}P NMR (D_2O) δ 38.0; IR data (cm^{-1}) 3100 w, 1630 s, 1600 s, 1575 m, 1330 w, 1300 w, 1200 m, 1090 s, 1055 s, 962 s, 831 w, 796 m, 722 m, 645 m, 603 m, 560 w, 505 w; FAB/MS M^+ = 558. Cryoscopic molecular weight in H_2O = 590 ± 60 g/mol. Anal. Calcd for $C_{20}H_{22}N_5O_6MoP$: C, 43.17; H, 3.96; N, 12.59; P, 5.58; MW = 557. Found: C, 43.14; H, 4.00; N, 12.64; P, 5.60.

Titration of 2'-Deoxyribonucleotides with Cp_2MoCl_2. The coordination of aqueous Cp_2MoCl_2 to 2'-deoxymononucleotides was further investigated in solution by mixing various ratios of **1** with mononucleotides (pD = 7.4) and monitoring the resulting reactions by ^1H and ^{31}P NMR spectroscopy. In a typical experiment, three Schlenk tubes were each charged with 0.30 mmol of the disodium salt of a 2'-deoxyribonucleotide. Each tube was then taken into the glovebox and charged with the appropriate amount of **1** to attain the desired **1**/mononucleotide ratio (0.2–1.0 equiv). On the Schlenk line, the tubes were charged with 2.0 mL of D_2O under a nitrogen flush and allowed to stir for an hour before the pD of the solutions was adjusted to 7.2–7.4 with concentrated aqueous NaOD. A 1.0-mL aliquot of each solution was transferred to a 5-mm NMR tube under a nitrogen flush, and ^1H and ^{31}P NMR spectra were immediately recorded. In order to verify that equilibrium had already been established, another set of spectra was recorded 24 h later to ensure that no spectroscopic changes had occurred.

Competition for Aqueous Cp_2MoCl_2 by 2'-Deoxymononucleoside-5'-monophosphates. In the glovebox, a Schlenk tube was charged with 0.13 mmol of the disodium salt of a 2'-deoxymononucleotide, and a second Schlenk tube was charged with 0.12 mmol of $Na_2(5'\text{-dGMP})$ and 0.070 mmol of Cp_2MoCl_2. Next, the Schlenk tubes were each charged with 2.0 mL of D_2O under an N_2 flush, and the solutions in the two tubes were stirred for 30 min before they were combined (pD = 7.6–7.8). A 1.0-mL aliquot of the resulting solution was then transferred to a 5-mm NMR tube under N_2 flush, and an ^1H NMR spectrum was immediately recorded using a 20-s pulse delay. A second set of experiments was performed wherein one Schlenk tube was charged with $Na_2(5'\text{-dGMP})$ and the other tube contained the disodium salt of a mononucleotide and Cp_2MoCl_2.

pD Titration of $Cp_2Mo(5'\text{-dAMP})$ (6) and $Cp_2Mo(5'\text{-dCMP})$ (7a and 7b). pD titrations of the Cp_2Mo(nucleotide) complexes used to probe the site of mononucleotide coordination were carried out in 5-mm NMR tubes where the pD was sequentially varied with 1–5 μL aliquots of concentrated DCl or NaOD added under an argon flush. Chemical shifts were referenced to a D_2O solution of Me_4NCl (3.18 ppm) in a 1-mm coaxial insert. The cyclopentadienyl resonances remained magnetically nonequivalent over the entire pH range. The reported titration pD values are uncorrected for deuterium isotope effects since pK_a's measured in H_2O and D_2O are virtually identical.[21]

Crystallographic Study of $[Cp_2Mo(9\text{-methyladenyl})][PF_6]$ (3a). This compound crystallizes as red cubes in the triclinic space group $P\bar{1}$ with a = 10.682 (3) Å, b = 11.619 (5) Å, c = 7.701 (5) Å, α = 106.93 (4)°, β = 96.32 (3)°, γ = 86.98 (3)°, Z = 2 at 168 (1) K. Crystallographic data were collected on a single crystal of **3a** mounted on a glass fiber by Molecular Structure Corporation (College Station, TX). All data ($4° < 2\theta < 55°$) were collected at room temperature on a Rigaku AFC6 diffractometer with Mo Kα radiation and a graphite monochromator using the ω-2θ technique (4150 unique reflections). Cell constants were obtained from a least-squares refinement using the setting angles of 25 carefully centered reflections in the range $24 < 2\theta < 32°$. Azimuthal scans of several reflections indicated no need for an absorption correction (crystal size: 0.30 × 0.20 × 0.15 mm; μ = 8.20 cm^{-1}; transmission factor = 0.89–1.00). The intensities of three representative reflections, which were measured after every 150 reflections, remained constant throughout the data collection indicating crystal and instrumental stability.

The structure of **3a** was solved by direct methods using a locally modified SHELX76 crystallographic program that first located the Mo and P atoms. The remaining non-hydrogen atoms were located by successive difference Fourier maps and refined to R = 10% with least-squares full-matrix refinement. The occupancies of the three orientations of the PF_6^- anion were refined until the late stages of the structure refinement. This gave a good indication of their distribution. In the last few cycles of refinement, a model was employed in which three different PF_6^- orientations sharing a common phosphorus atom were assigned occupancy factors 0.50, 0.25, and 0.25, respectively. Isotropic refinement of this model gave R = 7%. The refinement continued by assigning anisotropic temperature factors to all but the disordered fluorine atoms. Finally, the hydrogen atomc positions were calculated (assuming C–H = 0.95 Å) and included in the structure factor calculation but were not refined. The final refinement converged to R = 4.54% and R_w = 5.00%. In the last cycle of refinement, all parameter shifts were less than 10% of their estimated standard deviations (esd). Further details concerning the crystal characteristics and experimental methodology are summarized in Table I.

Table I. Data for Single-Crystal X-ray Analyses of $[Cp_2Mo(9\text{-methyladenyl})][PF_6]$ (**3a**), $[Cp_2Mo(1\text{-methylcytosyl})][PF_6]$ (**4**), and $[Cp_2Mo(5'\text{-dGMP})]_2$ (**5**)

formula	**3a** $C_{16}H_{16}N_5MoPF_6$	**4** $C_{15}H_{16}N_3OMoPF_6$	**5** $C_{40}H_{44}O_{14}N_{10}Mo_2P_2(H_2O)_{12.7}$
fw	519	495	1339
a, Å	10.682 (3)	11.703 (1)	10.690 (3)
b, Å	11.619 (5)	10.794 (2)	14.567 (5)
c, Å	7.701 (5)	14.416 (2)	9.298 (3)
α, deg	106.93 (4)	90.00	107.20 (2)
β, deg	96.32 (3)	111.28 (1)	99.22 (3)
γ, deg	86.98 (3)	90.00	77.62 (3)
Z	2	4	1
V, Å^3	908.6	1696.8	1344 (2)
space group	$P\bar{1}$	$P2_1/c$	$P1$
d_{calcd}, g/cm^3	1.73	1.77	1.65
cryst size, mm	0.30 × 0.20 × 0.15	0.40 × 0.20 × 0.05	0.43 × 0.38 × 0.28
radiation	Mo,Kα λ = 0.71073 Å	Mo,Kα λ = 0.71073 Å	Mo,Kα λ = 0.71069 Å
μ(Mo Kα), cm^{-1}	8.20	8.76	6.20
trans factor	0.89–1.00	0.84–1.00	0.76–1.00
$2\theta_{max}$, deg	55	55	55
scan type	ω-2θ	ω-2θ	ω-2θ
no. of unique data	4150	3813	6136
no. of data used ($F_o^2 > 3\sigma(F_o)^2$)	3614	3007	5491
no. of variables	280	262	727
$R(F)$	0.045	0.047	0.045
$R_w(F)$	0.050	0.052	0.062

Crystallographic Study of $[Cp_2Mo(1\text{-methylcytosyl})][PF_6]$ (4). This compound crystallizes as red plates in the monoclinic space group $P2_1/c$ with a = 11.703 (1) Å, b = 10.794 (2) Å, c = 14.416 (2) Å, β = 111.28 (1)°, and Z = 4 at 203 (1) K. Data collection for **4** utilized a Nonius CAD4 diffractometer and the procedures described for **3a** above (3813 unique reflections; crystal size: 0.40 × 0.20 × 0.05 mm). As a check on crystal and instrumental stability, three representative reflections were measured every 41 min. Absorption corrections were applied from calculated absorption curves (transmission factors ranged for 0.842 to 1.00); there was no evidence for crystal decomposition or extinction.

The Mo and P atoms were located from a Patterson map and then used as input for the phasing of a difference electron density Fourier map. The remaining non-hydrogen atoms were located using the same methodology described for **3a**. The final refinement converged to R = 4.71% and R_w = 5.24%. Further details on the crystallographic analysis are given in Table I.

Crystallographic Study of $[Cp_2Mo(5'\text{-dGMP})]_2$ (5). This compound crystallizes as green needles in the triclinic space group $P1$ with a = 10.690 (5) Å, b = 14.567 (3) Å, c = 9.298 (3) Å, α = 107.20°, β = 99.22 (3)°, γ = 77.63 (3)°, and Z = 1 at 153 K. Since the compound is optically active, the enantiomorphic space group $P1$ (no. 1) was assumed to be correct. Crystallographic data were collected on a single crystal of **5** mounted anaerobically in a 0.4-mm capillary tube. All data ($4° < 2\theta < 55°$) were collected as described for **4** above using the ω-2θ technique (6136 unique reflections; crystal size = 0.43 × 0.38 × 0.28 mm). Accurate unit cell parameters were obtained by least-squares refinement of the setting angles for 25 high-angle reflections. The intensities of four standard reflections were monitored every three hours of X-ray exposure showing no significant variations. Empirical absorption corrections were applied from Ψ scans of eight Bragg reflections (transmission factors ranged from 0.76 to 1.00); there was no evidence of crystal decomposition.

The structure solution for **5** was carried out with the TEXSAN crystallographic software package. A satisfactory phasing pattern was obtained by placing one of the molybdenum atoms at the origin. The remaining non-hydrogen atoms were located by successive difference Fourier maps and refined to R = 4.5% using a least-squares full-matrix refinement with anisotropic parameters for all non-hydrogen atoms. The choice between the two possible enantiomeric structures was made on the basis of the known absolute configuration of the deoxyribose unit. High

(21) Scheller, K. H.; Scheller-Krattinger, V.; Martin, R. B. *J. Am. Chem. Soc.* **1981**, *103*, 6833–6839.

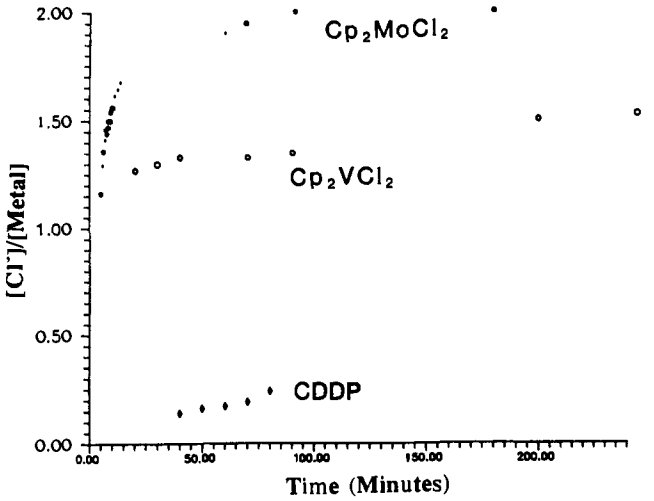

Figure 1. Concentration of free chloride/concentration of metal vs time (from time of mixing) plot for aqueous solutions of Cp_2MoCl_2 (*), Cp_2VCl_2 (O) (ref 12) and cisplatin (CDDP (◊) (ref 12). All solutions are approximately the same concentration in metal, 0.318 M in KNO_3, and at 37 °C.

thermal parameters suggested that the position of the oxygen atom in the W(13) water molecule (O(W13)) was only partially occupied, and consequently the population parameter of O(W13) was refined, ultimately reaching a value of 0.71 (2). The final Fourier difference map was virtually featureless with the highest peak being 0.52 eÅ^{-3}. Additional experimental details are given in Table I.

Molecular Graphics Studies. Docking studies of Cp_2Mo^{2+} to the d(ApGpGpT)/d(TpCpCpT) duplex were carried out using the oligonucleotide option of the BIOGRAF software package,[22] implemented on a microVAX 2000 with an Evans and Sutherland PS390 graphics system. The duplex structure was first energy minimized. Then using metrical parameters from the $[Cp_2Mo(5'\text{-dGMP})]_2$ and other crystal structures (Mo–N = 2.30 Å, ∠N–Mo–N = 91°), docking studies were carried out with respect to N7 binding at the d(pGpG) portion of the oligonucleotide.

Results

The objective of this investigation was the solution and solid-state characterization of aqueous Cp_2MoCl_2-nucleobase/nucleotide coordination chemistry. We begin with a discussion of Cp_2MoCl_2 aquation chemistry, followed by NMR spectroscopic studies of Cp_2MoCl_2(aq) reactivity with respect to alkylated nucleobases. In support of the solution spectroscopic studies, the diffraction-derived molecular structures of $[Cp_2Mo(9\text{-methyladenyl})][PF_6]$ (**3a**) and $[Cp_2Mo(1\text{-methylcytosyl})][PF_6]$ (**4**) are presented. We then discuss Cp_2MoCl_2(aq)-2′-deoxymononucleotide coordination chemistry in solution and the crystal structure of $[Cp_2Mo(2'\text{-deoxyguanosine-5}'\text{-monophosphate}]_2$ (**5**).

Aqueous Chemistry of Cp_2MoCl_2. The protonolytic loss of cyclopentadienyl ligands in Cp_2MX_2 complexes is conveniently and quantitatively monitored by ^{1}H NMR. Thus, protonolysis is accompanied by diminution (versus an internal standard) of Cp_2M resonances (observable for diamagnetic complexes) and the appearance of CpH signals (solubility ≈ 4 mM in H_2O) or those of CpH-derived products. In the case of Cp_2TiCl_2 and Cp_2ZrCl_2, rapid M–Cp protonolysis is observed.[12] In contrast, unbuffered aqueous Cp_2MoCl_2 solutions (10 mM, 37 °C) evidence no (<3% relative to internal DSS) Mo–Cp protonolysis for periods up to 4 weeks, while solutions at physiological pH (pD 7.4) and chloride concentration ([NaCl] = 0.103 M) exhibit no (<3% relative to internal DSS) Mo–Cp protonolysis for periods up to 2 weeks. The ^{1}H NMR spectrum of aqueous Cp_2MoCl_2 at pD 7.4 reveals one major cyclopentadienyl resonance at 5.97 ppm with a minor feature (~5% by integration) at 5.85 ppm. In contrast to aqueous Cp_2MoCl_2, the Mo–Cp ligation is less stable in dry Me_2SO-d_6 as indicated by the appearance of traces of free cyclopentadiene (5% relative to the C_5H_5–Mo resonance at 5.65 ppm) within 24 h. A similar, small cyclopentadienyl loss (3%) was also noted for a Me_2SO-d_6/saline solution of Cp_2VCl_2 after 1.5 h.[12]

Table II. ^{1}H NMR Spectroscopic Data[a] for $[Cp_2Mo(9\text{-methyladenyl})][PF_6]$ (**3a** and **3b**) and $[Cp_2Mo(1\text{-methylcytosyl})][PF_6]$ (**4**)

compound	H2[b]	H8[b]	C_5H_5[b]	N6H[b]
9-methyladenine (9-MeAd)	8.14 (1)	8.08 (1)		7.17 (2)
$[Cp_2Mo(9\text{-MeAd})]PF_6$ (**3a**)	7.64 (1)	8.00 (1)	5.84 (10)	6.90 (1)
$[Cp_2Mo(9\text{-MeAd})]PF_6$ (**3b**)	8.16 (1)	8.32 (1)	5.88 (10)	6.90 (1)
compound	H6[b]	H5[b]	C_5H_5[b]	N4H[b]
1-methylcytosine (1-MeCyt)	7.54 (1)	5.58 (1)		6.92 (2)
$[Cp_2Mo(1\text{-MeCytl})]PF_6$ (**4**)	7.55 (1)	5.16 (1)	5.77 (10)	6.42 (1)

[a] ^{1}H NMR chemical shift vs TMS in Me_2SO-d_6. [b] Number in parentheses denotes number of protons per formula unit by integration.

In contrast to the hydrolytic stability of the cyclopentadienyl ligands, chloride loss from Cp_2MoCl_2(aq) is both rapid and extensive. By the time Cp_2MoCl_2 dissolution in H_2O (37 °C) is complete, the $[Cl^-]/[Mo]$ ratio is already 1.2 (1) and asymptotically approaches 1.95 (5) within 60 min (Figure 1). Thus, compared to cisplatin and Cp_2VCl_2, the equilibrium for the chloride hydrolysis of Cp_2MoCl_2 lies very far to the right and is approached far more rapidly. The initial portion of the free chloride/metal versus time plot was found to be approximately linear, and an estimation of the half-life for the loss of the second chloride ion (6.7 (2) min) was determined by fitting a least-squares line to the initial data. The rapid and complete chloride loss for Cp_2MoCl_2(aq), not surprisingly, is unaffected in a 0.318 M KNO_3 ionic strength buffer, and is too rapid to measure when the pH is brought to 7.4 with NaOH.

The titration of aqueous Cp_2MoCl_2 with NaOH reveals two deprotonations with $pK_a(1) = 5.5$ (3) and $pK_a(2) = 8.5$ (3). Hence, using the classical hydrolysis model for cisplatin[23] and Cp_2VCl_2,[12] the hydrolytic steps of Cp_2MoCl_2 can be tentatively formulated as in eqs 1–4 where the rapid chloride loss proceeds to completion. These titrimetric data argue that at physiological pH, the predominant Cp_2MoCl_2(aq) solution species present is

$$Cp_2MoCl_2 + H_2O \rightleftarrows Cp_2Mo(H_2O)Cl^+ + Cl^- \quad (1)$$

$$Cp_2Mo(H_2O)Cl^+ + H_2O \rightleftarrows Cp_2Mo(H_2O)_2^{2+} + Cl^- \quad (2)$$

$$Cp_2Mo(H_2O)_2^{2+} + OH^- \rightleftarrows Cp_2Mo(OH)(OH_2)^+ \quad (3)$$

$$Cp_2Mo(OH)(OH_2)^+ + OH^- \rightleftarrows Cp_2Mo(OH)_2 \quad (4)$$

predominantly the monocation, $Cp_2Mo(OH)(H_2O)^+$.[24] In agreement with these observations, it was also found that $Cp_2Mo(OH)(H_2O)^+B(C_6H_5)^-_4 \cdot {}^1/_2H_2O$ could be precipitated from such solutions in high yield at pH 7.4 (see Experimental Section for characterization data). The exact structural nature of this complex (beyond magnetically equivalent Cp ligands) remains to be elucidated, and the presence of oligomeric species cannot be ruled out.

Molybdenocene Coordination to Nucleobases. The interaction of the representative purine and pyrimidine nucleobases 9-methyladenine and 1-methylcytosine with Cp_2MoCl_2(aq) was studied in solution by NMR. Methylated nucleobases were chosen to more closely simulate the native deoxyribose N-functionalized coordination environments. The coordination modes were investigated in both aqueous media and in Me_2SO-d_6 (to observe exchangeable amino protons). At room temperature, all nu-

(22) Mayo, S. L.; Olafson, B. D.; Goddard, W. A., III, *BIOGRAF Version 2.1 Reference Manual*; BioDesign, Inc., Pasadena, CA, 1990, Chapter 19.1–19.58.

(23) (a) Lippard, S. J. *Science* **1982**, *218*, 1075–1082 and references therein. (b) Lee, K. W.; Martin, D. S., Jr. *Inorg. Chim. Acta* **1976**, *17*, 105–110, and references therein.

(24) (a) That $Cp_2Mo{=}O$ could be one of the aqueous species at pH 7.4 is highly unlikely as it is reported to be insoluble in H_2O and is prepared by the addition of 25 equiv of NaOH to Cp_2MoCl_2.[24b] (b) Green, M. L. H.; Lynch, A. H.; Swanwick, M. G. *J. Chem. Soc., Dalton Trans.* **1972**, 1445–1447.

Table V. Selected Bond Distances (Å)[a] and Angles (deg)[a] for [Cp_2Mo(9-methyladenyl)][PF_6] (**3a**)

atom 1	atom 2	distance	atom 1	atom 2	distance
Mo	N1	2.173 (3)	C(11)	C(12)	1.417 (7)
Mo	N6	2.145 (3)	C(12)	C(13)	1.409 (7)
Mo	C(11)	2.348 (5)	C(13)	C(14)	1.440 (8)
Mo	C(12)	2.270 (4)	C(14)	C(15)	1.425 (10)
Mo	C(13)	2.258 (4)	C(15)	C(11)	1.381 (9)
Mo	C(14)	2.286 (5)	C(21)	C(22)	1.396 (6)
Mo	C(15)	2.346 (5)	C(22)	C(23)	1.419 (7)
Mo	C(21)	2.319 (4)	C(23)	C(24)	1.410 (7)
Mo	C(22)	2.359 (4)	C(24)	C(25)	1.415 (8)
Mo	C(23)	2.346 (5)	C(25)	C(21)	1.427 (5)
Mo	C(24)	2.307 (5)			
Mo	C(25)	2.253 (4)	Mo	Cg(av)	1.97 (1)
C6	N6	1.314 (5)	C6	N1	1.382 (5)
C2	N1	1.336 (5)	C2	N3	1.324 (5)
C4	N3	1.355 (5)	C4	C5	1.391 (5)
C4	N9	1.374 (5)	C5	C6	1.409 (5)
C5	C7	1.382 (5)	C8	N7	1.310 (6)
C8	N9	1.366 (5)	C9	N9	1.450 (6)

atom 1	atom 2	atom 3	angle	atom 1	atom 2	atom 3	angle
Cg1	Mo	Cg2	135.3	N6	Mo	N1	60.9 (1)
Cg1	Mo	N1	109.1	Cg2	Mo	N1	109.6
Cg1	Mo	N6	106.2	Cg2	Mo	N6	111.7
C(11)	C(12)	C(13)	107.2 (5)	C(24)	C(25)	C(21)	108.8 (4)
C(12)	C(13)	C(14)	108.9 (5)	C(25)	C(21)	C(22)	107.0 (4)
C(13)	C(14)	C(15)	105.3 (5)	C(22)	C(23)	C(24)	108.2 (4)
C(14)	C(15)	C(11)	109.8 (5)	C(23)	C(24)	C(25)	107.1 (4)
C(15)	C(11)	C(12)	108.7 (5)	C(21)	C(22)	C(23)	108.9 (4)
N3	C4	N9	126.0 (4)	Mo	N6	C6	97.0 (9)
N3	C4	C5	128.4 (4)	Mo	N1	C6	93.6 (9)
C5	C4	N9	105.6 (3)	N6	C6	C5	135.8 (6)
C5	N7	C8	103.6 (3)	N1	C6	C5	115.7 (4)
N7	C8	N9	114.5 (3)	N6	C6	N1	108.5 (3)
C4	C5	N7	110.8 (5)	N1	C2	N3	125.2 (4)
C4	C5	C6	115.6 (5)	C8	N9	C4	105.6 (3)
C6	C5	N7	133.6 (6)	C2	N3	C4	112.1 (3)
C8	N9	C9	127.3 (4)	N2	N1	C6	122.8 (5)

[a] Estimated standard deviations in the least significant figure are given in parentheses. Cg1 and Cg2 are centroids of rings composed of atoms C(10)–C(15) and C(21)–C(25), respectively.

cleobase protons can be readily assigned from well-documented correlations[25] and selective deuteration experiments.[20b] In addition, the nucleobase complexes can be formed on a preparative scale (eq 5) and isolated as PF^-_6 salts for elemental analysis, additional spectroscopy, and diffractometric characterization (vide infra). Control NMR experiments showed **3** and **4** to be spectroscopically indistinguishable from the cationic complexes formed in aqueous solution upon initial mixing.

$$Cp_2MoCl_2(aq) + BH + PF^-_6 \xrightarrow[18h]{\text{pH 7.4}} Cp_2MoB^+PF^-_6 + H^+ + 2Cl^- \quad (5)$$

3a, BH = 9-methyladenine
3b, BH = 9-methyladenine
4, BH = 1-methylcytosine

NMR data for **3** and **4** are compiled in Table II. The initial reaction of $Cp_2MoCl_2(aq)$ with 9-methyladenine (see Experimental Section for details) yields two [Cp_2Mo(9-methyladenyl)][PF_6] isomers (**3a**, 90%; **3b**, 10%). Complex **3a** can be quantitatively converted to **3b** by heating **3a** at 80 °C for 1 week (Figure 2), suggesting that **3a** is a kinetic product and that **3b** is more thermodynamically stable. The singlet cyclopentadienyl ^1H NMR resonances in **3a** and **3b** indicate both complexes have magnetically equivalent Cp ligands. Furthermore, the chemical shift displacements for the amino proton as well as H2 and H8 in **3a** and **3b** relative to 9-methyladenine (Table II) suggest $HN6^-/N1$ and $HN6^-/N7$ chelation modes, respectively. This strained, four-membered chelation mode and magnetically equivalent cyclopentadienyl ligation in **3a** is confirmed by X-ray diffraction studies (vide infra) that reveal a mononuclear Cp_2Mo(9-methyladenyl)$^+$

(25) Davies, D. B. *Prog. NMR Spectrosc.* **1978**, *12*, 135–225, and references therein.

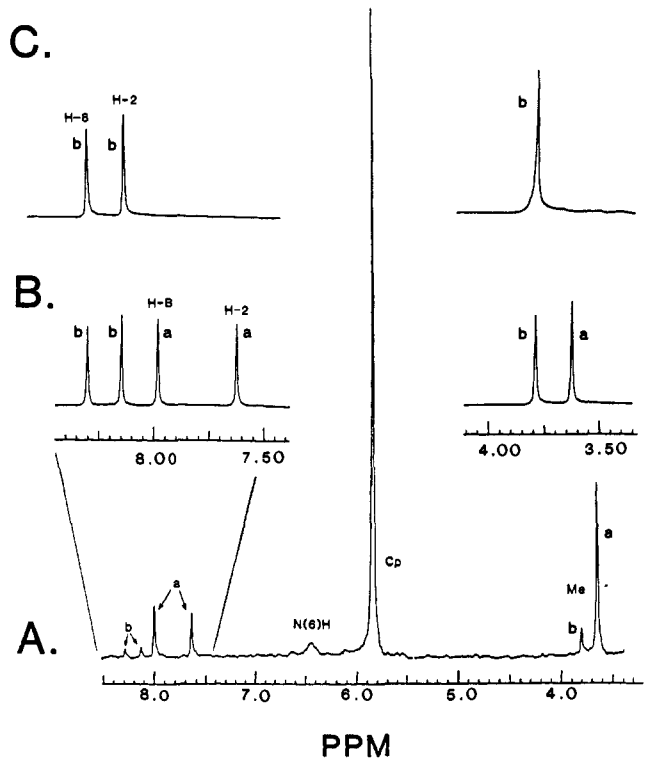

Figure 2. Isomerization of [Cp_2Mo(9-methyladenyl)]$^+PF^-_6$ isomer **3a** to isomer **3b** (see eq 6 in text) as monitored by ^1H NMR in Me_2SO-d_6 at 80 °C: (A) after 1 day, (B) after 4 days, and (C) after 8 days. The labels **a** and **b** refer to resonances of **3a** and **3b**, respectively.

adduct with the 9-methyladenine plane situated in the equatorial girdle of the Cp_2Mo^{2+} moiety. Along with the established monomeric nature of **3b**, the **3a** → **3b** isomerization can then be described as in eq 6.

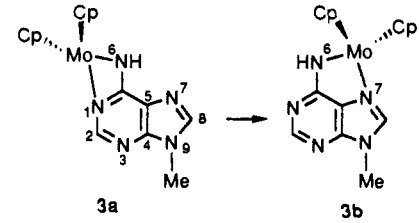

(6)

The reaction of **1** with 1-methylcytosine yields a single [Cp_2Mo(1-methylcytosyl)][PF_6] product (**4**) with ^1H NMR spectral parameters (Table II) that indicate N4-H deprotonation and magnetically equivalent Cp ligands. Crystallographic studies of **4** (vide infra) indeed show that the Cp_2Mo^{2+} moiety is σ-bonded to N4 and N3 of the same 1-methylcytosine ligand and that the nucleobase ligand is situated in the plane bisecting the ring centroid–Mo–ring centroid angle (the "equatorial girdle").

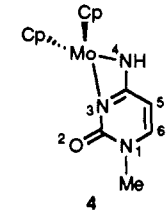

Solid-State Structures of [Cp_2Mo(9-methyladenyl)][PF_6] (3a) and [Cp_2Mo(1-methylcytosyl)][PF_6] (4). X-ray diffraction reveals that single crystals of **3a** and **4** are composed of discrete mononuclear [Cp_2Mo(nucleobase)]$^+$ cations and well-separated PF^-_6 counterions. To a good approximation, the anion has O_h symmetry, and the Mo(IV) ion adopts the familiar "clamshell" ge-

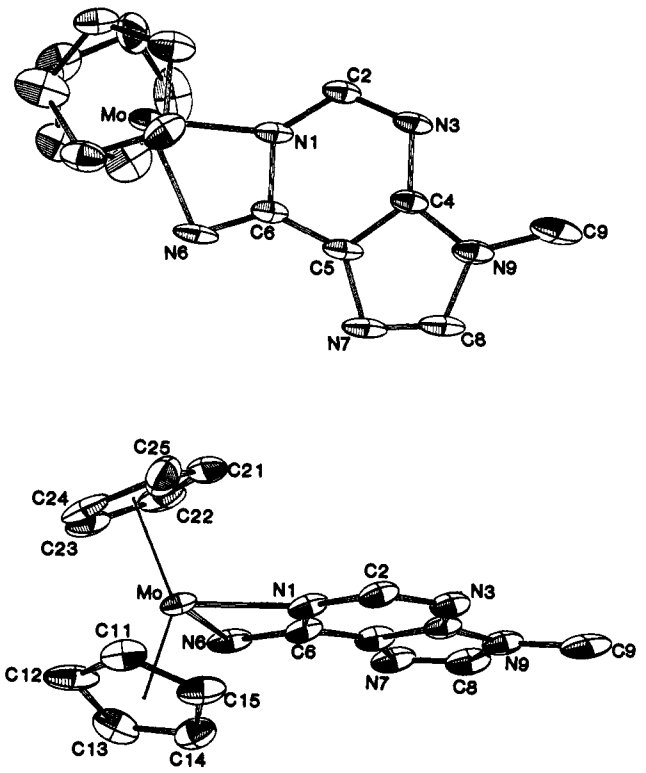

Figure 3. Perspective views of the non-hydrogen atoms of $[Cp_2Mo(9\text{-methyladenyl})]^+PF^-_6$ (**3a**) showing the cation portion. Ellipsoids are drawn to include 30% probability. Important bond distances (Å) and angles (deg) are as follows: Mo–N1 = 2.173 (3), Mo–N6 = 2.146 (3), C6–N1 = 1.314 (5), Mo–ring centroid = 1.97 (1) (av), ∠N1–Mo–N6 = 60.9, ∠N6–C6–N1 = 108.5 (3), ∠ring centroid–Mo–ring centroid = 135.3, ∠Mo–N6–C6 = 97.0 (9), and ∠Mo–N1–C6 = 93.6 (9).

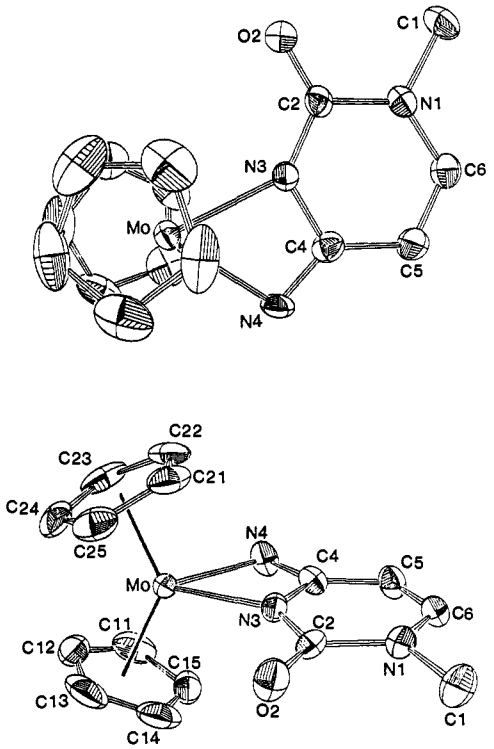

Figure 4. Perspective views of the non-hydrogen atoms of $[CpMo(1\text{-methylcytosyl})]^+PF^-_6$ (**4**) showing the cation portion. Ellipsoids are drawn to include 30% probability. Important bond distances (Å) and angles (deg) are as follows: Mo–N3 = 2.130 (5), Mo–N4 = 2.140 (5), C4–N4 = 1.291 (7), C4–N4 = 1.363 (7), Mo–centroid (av) = 1.959 (8), ∠N4–Mo–N3 = 59.9 (1), ∠ring centroid–Mo–ring centroid = 136.5, ∠N3–C4–N4 = 106.8 (5), ∠Mo–N4–C4 = 97.6 (4), and ∠Mo–N3–C4 = 95.8 (3).

Table VI. Selected Bond Distances (Å)[a] and Angles (deg)[a] for $[Cp_2Mo(1\text{-methylcytosyl})][PF_6]^-$ (**4**)

atom 1	atom 1	distance	atom 1	atom 2	distance
Mo	N3	2.130 (5)	C(11)	C(12)	1.381 (12)
Mo	N4	2.140 (5)	C(12)	C(13)	1.389 (13)
Mo	C(11)	2.257 (7)	C(13)	C(14)	1.351 (13)
Mo	C(12)	2.291 (7)	C(14)	C(15)	1.390 (13)
Mo	C(13)	2.328 (7)	C(15)	C(11)	1.432 (12)
Mo	C(14)	2.313 (7)	C(21)	C(22)	1.428 (12)
Mo	C(15)	2.259 (7)	C(22)	C(23)	1.393 (12)
Mo	C(21)	2.249 (7)	C(23)	C(24)	1.382 (11)
Mo	C(22)	2.279 (7)	C(24)	C(25)	1.408 (12)
Mo	C(23)	2.333 (7)	C(25)	C(21)	1.442 (12)
Mo	C(24)	2.346 (7)			
Mo	C(25)	2.282 (7)	Mo	Cg(av)	1.959 (8)
C4	N4	1.291 (7)	C4	N3	1.363 (7)
C5	C4	1.413 (8)	C5	C6	1.336 (9)
C6	N1	1.375 (7)	N1	C1	1.458 (7)
N1	C2	1.402 (7)	C2	N3	1.359 (7)
C2	O2	1.216 (7)			

atom 1	atom 2	atom 3	angle	atom 1	atom 2	atom 3	angle
Cg1	Mo	Cg2	136.5	Mo	N4	C4	97.6 (4)
N4	Mo	N3	59.9 (1)	Mo	N3	C4	95.8 (3)
N4	Mo	Cg1	110.9	N4	Mo	Cg2	108.2
N3	Mo	Cg1	108.0	N4	Mo	Cg2	108.1
C(11)	C(12)	C(13)	110.1 (7)	C(21)	C(22)	C(23)	106.5 (7)
C(12)	C(13)	C(14)	107.7 (8)	C(22)	C(23)	C(24)	110.0 (7)
C(13)	C(14)	C(15)	109.5 (8)	C(23)	C(24)	C(25)	109.4 (7)
C(14)	C(15)	C(11)	107.5 (7)	C(24)	C(25)	C(21)	105.8 (7)
C(15)	C(11)	C(12)	105.1 (7)	C(25)	C(21)	C(22)	108.3 (7)
N3	C4	N4	106.8 (5)	N1	C2	N3	114.1 (5)
N4	C4	C5	132.8 (6)	C4	C5	C6	116.1 (5)
C5	C6	N1	122.8 (5)	C6	N1	C2	120.6 (5)
C1	N1	C2	117.1 (5)	N1	C2	O2	121.8 (5)
O2	C2	N3	124.1 (5)	C2	N3	C4	124.2 (5)
N3	C4	C5	120.4 (5)	C1	N1	C6	120.6 (5)

[a] Standard deviations and definitions of Cg1 and Cg2 are as described in Table V.

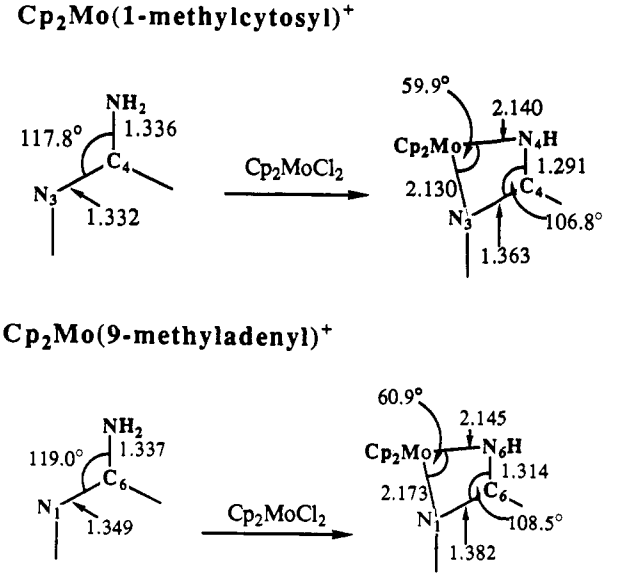

Figure 5. Comparison of metrical parameters for Mo–nucleobase chelation ion $[Cp_2Mo(9\text{-methyladenyl})]^+PF^-_6$ (**3a**) and $[Cp_2Mo(1\text{-methylcytosyl})]^+PF^-_6$ (**4**).

ometry found in other Cp_2MoX_n complexes ($n = 2$,[26] $n = 1$[27]) with each Mo(IV) ion π-bonded to two staggered η^5-C_5H_5 ligands and

(26) (a) Calhorda, M. J.; de C. T. Carrondo, M. A. A. F.; Garcia, M. H.; Hursthouse, M. G. *J. Organomet. Chem.* **1988**, *342*, 209–214. (b) Calhorda, M. J.; de C. T. Carrondo, M. A. A. F.; Dias, A. R.; Domingos, A. M. T.; Duarte, M. T. L. S.; Garcia, M. H.; Romao, C. C. *J. Organomet. Chem.* **1987**, *320*, 63–81. (c) de C. T. Carrondo, M. A. A. F.; Calhorda, M. J.; Hursthouse, M. G. J. *Acta Crystallogr.* **1987**, *C43*, 880–883. (d) de C. T. Carrondo, M. A. A. F.; Domingos, A. M. T. S. *J. Organomet. Chem.* **1983**, *253*, 53–63. (e) Forder, R. A.; Gale, G. D.; Prout, C. K. *Acta Crystallogr.* **1975**, *B31*, 297–299. (f) Prout, C. K.; Cameron, T. S.; Forder, R. A.; Critchley, S. R.; Denton, B.; Rees, G. V. *Acta Crystallogr.* **1974**, *B30*, 2290–2304.

σ-bonded to two nitrogen atoms of the coordinated nucleobase. Atomic positions involving non-hydrogen atoms for **3a** and **4** are given in Tables III and IV, respectively. The hydrogen atoms of the cyclopentadienyl and nucleobase ligands were not located. Selected bond lengths and angles for **3a** and **4** are listed in Tables V and VI, respectively. Perspective views of **3a** and **4** are shown in Figures 3 and 4, respectively, with corresponding drawings in Figure 5 that compare metrical parameters involved in Cp_2Mo chelation.

$(C_5H_5)_2Mo(N)_2$ Geometries. The η^5-C_5H_5 ligation in **3a** and **4** is similar to that found in other Cp_2MoX_2 complexes, with Mo–Cg = 1.97 (1) (**3a**) and 1.96 (1) (**4**) Å, Mo–C(av) = 2.309 (4) (**3a**) and 2.294 (7) (**4**) Å, C–C(av) = 1.407 (9) (**3a**) and 1.407 (9) (**4**) Å. In comparison, for Cp_2MoCl_2,[26f] Mo–Cg = 1.97 (1), Mo–C(av) = 2.30 (1), C–C(av) = 1.385 (5) Å. The present ring centroid–Mo–ring centroid angles of 135.3° (**3a**) and 136.5° (**4**) can be compared to those in Cp_2MoX_n complexes such as $[Cp_2MoO_2PO_2MoCp_2][PF_6]$[27e] (134.3°), $[Cp_2Mo(L\text{-proline})][PF_6]$[27d] (135.6°), and $[Cp_2Mo(2\text{-HPy})][PF_6]$[27a] (134.1°; HPy represents a 2-oxypyridine chelated to Mo via O2 and N1).

The coordination positions in the Cp_2Mo equatorial girdle are occupied by N6 and N1 in **3a** and by N4 and N3 in **4**. The Mo–NH(exocyclic) bond distances in **3a** and **4** are essentially identical (2.145 (3) and 2.140 (5) Å, respectively), while the Mo–N(endocyclic) distance in **3a**, 2.173 (3) Å, is significantly longer than that in **4**, 2.130 (5) Å. These bond distances agree favorably with Mo(IV)–N distances of 2.139 (11) Å in $[Cp_2Mo(2\text{-HPy})][PF_6]$[27a] 2.160 (8) (Mo–N2) and 2.142 (9) (Mo–N1) Å in $[Cp_2Mo(2\text{-aminopyridine})][PF_6]$ ($[Cp_2Mo(NC_5H_4)\text{-NH}][PF_6]$),[27a] and 2.166 (3) and 2.157 (3) Å in $Cp_2Mo(pyrazole)_2$ ($Cp_2Mo(N_2C_3H_3)_2$).[26d] The N(exocyclic)–Mo–N(endocyclic) bond angle decreases dramatically from the Cl–Mo–Cl angle of 82.2° in Cp_2MoCl_2[26f] to 60.9 (1)° and 59.9 (1)° for **3a** and **4**, respectively. The acute N–Mo–N angles in **3a** and **4** are comparable to several Cp_2MoX_n systems with constricted L–Mo–L ligation such as in $Cp_2Mo(SO_4)$[27b] (66.1 (2)°), $[Cp_2Mo(2\text{-aminopyridine})][PF_6]$,[27a] (59.8 (3)°) and $[Cp_2Mo(2\text{-HPy})][PF_6]$ (61.2°).[27a]

Purine and Pyrimidine Geometries in $[Cp_2Mo(9\text{-methyladenyl})][PF_6]$ (3a) and $[Cp_2Mo(1\text{-methylcytosyl})][PF_6]$ (4). The most obvious structural changes in the coordinated nucleobases lie in the N(endocyclic)–αC–N(exocyclic) bond angles in the four-membered chelate rings. Relative to the free nucleobase, this angle for both **3a**[28] and **4**[29] is compressed by 11° toward the molybdenum center and is accompanied by an 11° expansion in the corresponding N6–C6–C5[28] (**3a**) and N4–C4–C5[29] (**4**) bond angles (Figure 5). In order to accommodate these structural changes, there are additional bond angle alterations within the nucleobase molecules. The 4° increase in ∠C6–N1–C2 and ∠C4–N3–C2 for **3a** and **4**,[30] respectively, is offset by a 4° decrease at the adjacent C2 position. The observed bond length alterations in **3a** and **4** upon coordination, as shown in Figures 4 and 5, are consistent with changes in charge delocalization in the nucleobases. Similar bond length alterations have been observed in $[Pt(NH_3)_2(OH)_2(1\text{-methylcytosyl-}N^4)_2](NO_3)_2$[31] and have been attributed to a decrease in the C4–N3 double bond character and an increase in the C4–N4 bond order. The remaining bond lengths and angles of the coordinated purine and pyrimidine in **3a** and **4** are, within experimental error, unchanged relative to the corresponding free ligands.

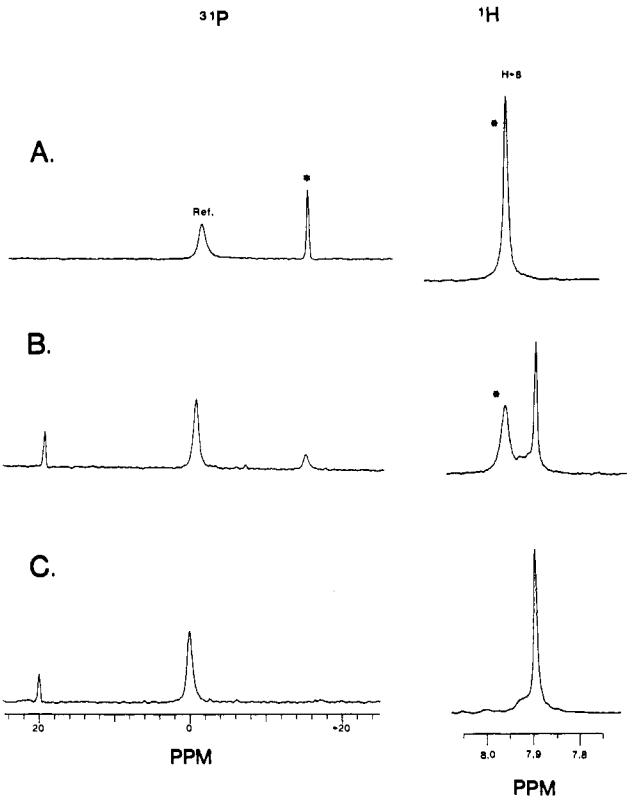

Figure 6. Titration of 2′-deoxyguanosine-5′-monophosphate (5′-dGMP) with Cp_2MoCl_2 in D_2O as monitored by 270 MHz ^1H and 161 MHz ^{31}P NMR spectroscopy. Asterisks (*) represent signals of free 5′-dGMP and ref = external ^{31}P reference signal. Phosphoric acid is at −18.5 ppm relative to the ^{31}P reference: (A) free 5′-dGMP, (B) 0.5 equiv of Cp_2MoCl_2, (C) 1.0 equiv of Cp_2MoCl_2.

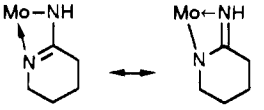

Cp_2MoCl_2 Coordination Chemistry with Deoxymononucleotides. Cp_2Mo–nucleotide interactions in D_2O were investigated by ^1H (270, 400 MHz) and ^{31}P(109, 161 MHz) NMR spectroscopy with reference to the coordination mode and the nucleotide conformation. Carbon-bound protons are readily observed by ^1H NMR in D_2O solution, and exchangeable amino protons are observable in Me_2SO-d_6. ^1H NMR assignments in the Cp_2Mo(nucleotide) complexes were aided by selective decoupling experiments as well as 2D COSY techniques that revealed little or no change in the chemical shifts of the deoxyribose protons. This precludes Mo(IV) coordination to, or deprotonation of, the deoxyribose rings. In addition, modified Karplus treatments of the intraribose coupling constants can afford insight into the relative populations of the various deoxyribose and phosphate backbone conformers. Thus, the relative population of the two common sugar conformers, C3′-endo and C2′-endo, can be determined from the observed magnitude of the $J_{H1'H2'}$, and equilibrium populations for the

(27) (a) Calhorda, M. J.; de C. T. Carrondo, M. A. A. F.; Da Costa, R. G.; Dias, A. R.; Duarte, M. T. L. S.; Hursthouse, M. B. *J. Organomet. Chem.* **1987**, *320*, 53–62. (b) Calhorda, M. J.; de C. T. Carrondo, M. A. A. F.; Dias, A. R.; Domingos, A. M. T. S.; Simoes, J. A. M.; Teixeira, C. *Organometallics* **1986**, *5*, 660–667. (c) Silavwe, N. D.; Chiang, M. Y.; Tyler, D. R. *Inorg. Chem.* **1985**, *24*, 4219–4221. (d) Prout, C. K.; Critchley, S. R.; Cannillo, E.; Tazzoli, V. *Acta Crystallogr.* **1977**, *B33*, 456–462. (e) Prout, C. K.; Couldwell, M. D.; Forder, R. A. *Acta Cryst.* **1977**, *B33*, 218–221. (f) Prout, C. K.; Allison, G. B.; Delbaere, L. T. J.; Gore, E. S. *Acta Crystallogr.* **1972**, *B28*, 3043–3056.

(28) (a) Bond angle N6–C6–N1 = 108.5 (3)° for **3a** compared to 119.0 (2)° in adenosine.[28b] N6–C6–C5 = 135.8 (6)° for **3a** and 123.4 (2)° for adenosine.[28b] (b) Taylor, R.; Kennard, O. *J. Mol. Struct.* **1982**, *78*, 1–28.

(29) (a) Bond angle N4–C4–N3 = 106.8 (5)° for **4** and 117.9 (2)° in 1-methylcytosine,[29b] and N4–C4–C5 = 132.8 (6°) for **4** and 121.8 (2) in 1-methylcytosine.[29b] (b) Rossi, M.; Kistenmacher, T. J. *Acta Crystallogr.* **1977**, *B33*, 3962–3965.

(30) It should be noted that the bond angle alterations in **3a** and **4** are also observed upon protonation of the pyrimidine endocyclic nitrogens, or upon deprotonation of the exocyclic NH2.[28b]

(31) Lippert, B.; Schöllhorn, H.; Thewalt, U. *J. Am. Chem. Soc.* **1986**, *108*, 6616–6621.

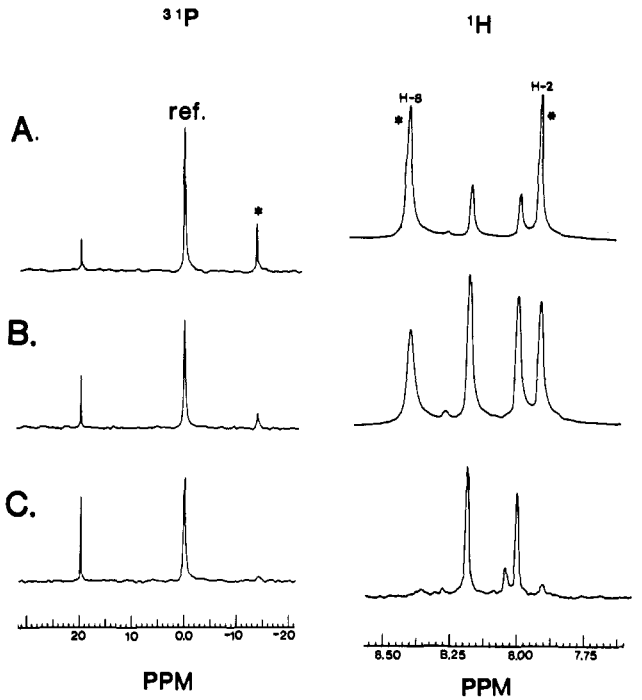

Figure 7. Titration of 2′-deoxyadenosine-5′-monophosphate (5′-dAMP) with Cp_2MoCl_2 in D_2O as monitored by 270 MHz ^1H and 109 MHz ^{31}P NMR spectroscopy. Asterisks (*) represent signals of free 5′-dAMP and ref = external ^{31}P reference signal. Phosphoric acid is at −18.5 ppm relative to the ^{31}P reference: (A) 0.25 equiv of Cp_2MoCl_2, (B) 0.5 equiv of Cp_2MoCl_2; and (C) 1.0 equiv of Cp_2MoCl_2.

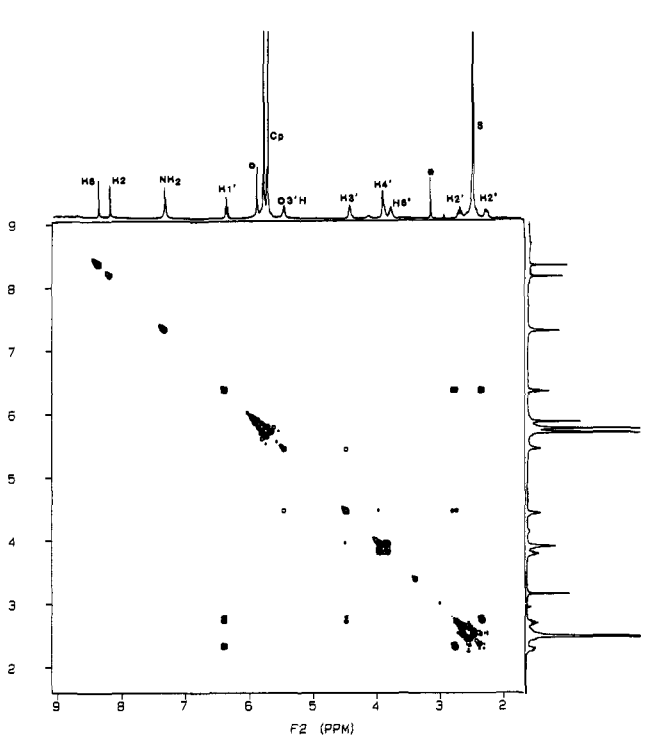

Figure 8. Two-dimensional COSY ^1H NMR spectrum (400 MHz) of Cp_2Mo(5′-dAMP), **6**, in Me_2SO-d_6. Assigned resonances are labeled along the F2 axis. The asterisk (*) represents a water impurity, S = the Me_2SO-d_6 solvent, and (O) = excess Cp_2MoCl_2 (aq).

gauche–gauche rotamer along the C5′–O5′[32,33] and C4′–C5′[32,33] bonds can be calculated from the respective vicinal coupling constants. Furthermore, nuclear Overhauser enhancement (NOE) studies were employed to assess the relative orientation of the nucleobase with respect to the ribose ring of the nucleotide. In the syn glycosidic conformation, the purine H8 is in close proximity to the deoxyribose H1′, resulting in a positive NOE. Likewise, in the anti conformation, a positive NOE should be detected between H8 and H2′ for purines.[34]

Nucleobase chemical shift data for the Cp_2Mo–nucleotide complexes are set out in Tables VII and VIII. That these Cp_2Mo–nucleotide complexes (pD 7.0) are stable in aqueous solution (pD 7.0) is demonstrated in the NMR by the negligible dimunition of the Cp_2Mo resonances and the absence of free cyclopentadiene over periods as long as 2 days. A complete compilation of the pertinent coupling constants with the derived conformational populations is given in the Supplementary Material.

$[Cp_2Mo(5'\text{-dGMP})]_2$ (5) and $Cp_2Mo(5'\text{-dAMP})$ (6). The titration of Na_2(5′-dGMP) and Na_2(5′-dAMP) with **1** in D_2O (Figures 6 and 7, respectively) reveals, on the NMR time scale, a nonlabile interaction with Cp_2MoCl_2(aq) that results in the ultimate formation of the 1:1 Cp_2Mo(nucleotide) adducts, $[Cp_2Mo(5'\text{-dGMP})]_2$ (**5**) and Cp_2Mo(5′-dAMP) (**6**). Spectroscopically characteristic features of $[Cp_2Mo(5'\text{-dGMP})]_2$ (**5**) and Cp_2Mo(5′-dAMP) (**6**) include characteristic 33 ppm downfield shifts of the ^{31}P signals[35] and a ~0.10 ppm upfield shift of the H8 resonances[36] (Table VII), thus indicating concurrent phosphate and nucleobase (N7)[37] coordination. This coordination mode also results in magnetically nonequivalent cyclopentadienyl resonances (Figure 8).[38] Further support for the proposed phosphate coordination in **5** and **6** is provided by the observation that the titration of sodium phenyl phosphate ($C_6H_5OP(O)(ONa)_2$) with **1** at pH 7.4 also results in a 30 ppm ^{31}P downfield displacement. The proposed coordination mode for **5** is confirmed in the solid state by diffraction studies (vide infra) that show Cp_2Mo^{2+} covalently bonded to 5′-dGMP N7 and O(phosphate) moieties. In agreement with the solution NMR results, a comparable 30 ppm downfield shift is observed in the solid-state ^{31}P spectrum of **5**. Attempts to grow diffraction quality crystals of **6** were unsuccessful.

In regard to the nucleotide conformation, NMR analysis of the sugar puckering in both **5** and **6** reveals an approximately equal distribution between the C3′-endo and C2′-endo conformers. Both **5** and **6** exist predominantly as the gauche–gauche rotamer about the O5′–C5′ and C5′–C4′ bond vectors. The NOE results for **5** suggest a syn glycosidic conformation since enhancements are observed between H1′ and H8 (9(1)%) and between H2′ and H8 (4(1)%). Likewise, the NOE observed between H8 and H2′ (9%(1)) and between H8 and H3′ (5%(1)) suggests an anti gly-

(32) (a) The conformational population in aqueous solution of the C3′-endo sugar conformer is expressed as:[32b] P(C3′-endo) = $(\sum J2'' - 6.9)/10.9$; $\sum J2'' = J_{H1'H2''} + J_{H2''H3'}$. (b) Altona, C. *Recueil Rev.* **1982**, *101*, 413–433.

(33) (a) Coupling constants cannot distinguish between gauche–trans and trans–gauche rotamers about the O5′–C5′ and C5′–C4′ bonds, and hence these two rotamers are treated as one conformer. The gauche–gauche conformational population about the O5′–C5′ bond is expressed as[32b] $(26.4 - \sum 5'P)/21.4$, where $\sum 5'P = J_{H5'P} + J_{H5''P}$ and the gauche–gauche conformation along the C5′–C4′ bond is expressed as $(13.7 - \sum 4'5')/9.7$, where $\sum 4'5' = J_{H4'H5'} + J_{H4'H5''}$. (b) It should be noted that these modified Karplus equations are derived for the free mononucleotides and may not explicitly account for any electronic effects of Cp_2Mo^{2+} coordination to N7 and O(phosphate).

(34) (a) Caradonna, J. P.; Lippard, S. J. *Inorg. Chem.* **1988**, *27*, 1454–1466. (b) Son, T.-D.; Guschlbauer, W.; Gueron, M. *J. Am. Chem. Soc.* **1972**, *94*, 7903–7911. (c) Reference 18.

(35) Gorenstein, D. G. In *Phosphorous-31 NMR. Principles and Applications*; Gorenstein, D. G., Ed.; Academic Press: Orlando, FL, 1984, pp 7–35.

(36) (a) Miller, S. K.; Marzilli, L. G. *Inorg. Chem.* **1985**, *24*, 2421–2425. (b) Marcelis, A. T. M.; van Kralingen, C. G.; Reedijk, J. *J. Inorg. Biochem.* **1980**, *13*, 213–222. (c) Downfield shifts of H8 are more typical for N7 coordination;[36a,b] however, models indicate that in the present case, H8 will be in the shielding region of the diamagnetically anisotropic Cp ligands. This can induce substantial upfield shifts.[36d] (d) Schock, L. E.; Brock, C. P.; Marks, T. J. *Organometallics* **1987**, *6*, 232–241.

(37) An additional note on N7 coordination for Cp_2Mo(5′-dAMP) (**6**): the chemical shifts in Me_2SO-d_6 of H8 (δ 8.30) and H2 (δ 8.14) in **3b** which, has an HN6$^-$/N7 chelation mode, are within 0.03 ppm of the H8/H2 chemical shifts of **6**.

(38) In the COSY spectrum of Cp_2Mo(5′-dAMP), the H2′ resonance can be assigned as downfield of the H2″ resonances. Molecular models show that rotation about glycosidic bond can readily place H2′ in the deshielding region of the nucleobase such that H2′ is downfield of H2″.

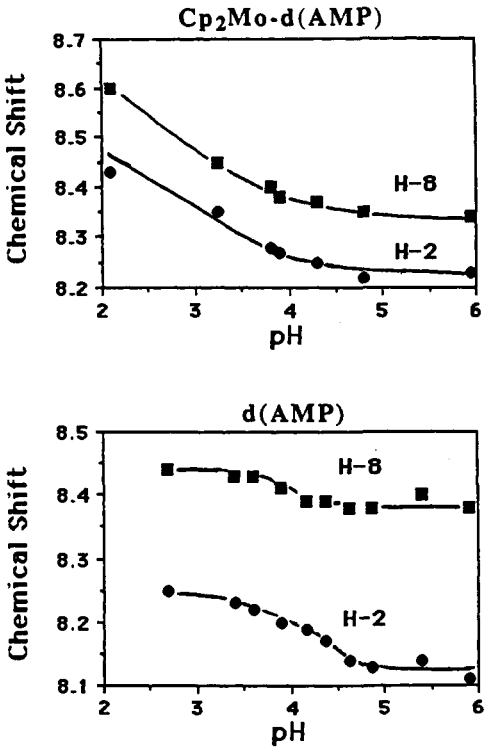

Figure 9. Chemical shifts vs pH of the nonexchangeable nucleobase protons, H8 and H2, of 5′-dAMP and Cp_2Mo(5′-dAMP) (6) in D_2O. The cyclopentadienyl ligands of 6 remain magnetically nonequivalent over the entire pH range.

cosidic conformation for **6**. Other nucleobase–ribose NOEs were too small (<1%) to be significant.

The Mo(IV) coordination to the nucleobase in Cp_2Mo(5′-dAMP) (**6**) was further examined via the pH dependence of the H8 and H2 chemical shifts. The sigmoidal curves shown in Figure 9 reveal the effects of protonation/deprotonation at the adenine N1 site. The downfield shifts of H2 and H8 in the low pH range reflect the redistribution of electron density in the adenine ring that results from protonation at N1. The stability of the Cp_2Mo(5′-dAMP) complexation during the pH titration is evidenced by the persistence of the Cp magnetic nonequivalence over the entire pH range. The changes in chemical shift of H8 and H2 at pH $\approx$ 3.0 are assigned to the protonation of N1 (pK_a = 3.8 in the uncoordinated base)[39] which argues against Cp_2Mo^{2+} coordination to N1. Furthermore, the $\sim$0.8 decrease in the pK_a of N1 in **6** is comparable to the $\sim$1.0 decrease observed in diethylenetriammine-(N7)-9-methyladenineplatinum(II) dichloride.[40] Thus, the elemental analysis, aqueous cryoscopy, and FAB/MS support for the monomeric nature of **6**, combined with the solution NMR results, suggest the structure shown below. Molecular models of the above structure show that Cp_2Mo^{2+} coordination to 5′-dAMP must indeed be accompanied by a shift toward the gauche–gauche rotamer about the C4′–C5′ and C5′–O5′ bond vectors, resulting in O5′ displacement above the deoxyribose ring. The other known mononuclear examples of metal–nucleotide adducts with N7/O(phosphate) chelation are

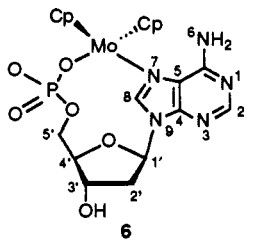

6

the structural formulations, on the basis of NMR data, of *cis*-$Pt(NH_2CH_3)_2$(5′-IMP)[41a] and $[RuCl(H_2O)(DMSO)_2$(5′-dGMP)].[41b] NMR and molecular mechanics analysis of a monomeric *cis*-$Pt(NH_3)_2$ (5′-GMP-N7, αPO) complex also reveals an exclusive preference for the gauche–gauche conformation about the O5′–C5′ and C5′–C4′ bonds, an anti glycosidic conformation, and a C3′-endo sugar puckering.[41c] Additional macrochelate complexes of purine 5′-nucleotides have been found that also involve N7 and phosphate coordination.[41d-h]

Cp_2Mo(5′-dCMP) (7a and 7b). The reaction of Na_2(5′-dCMP) with 1.2 equiv of **1** immediately yields two products, **7a** and **7b**, with ca. 75% conversion. The ratio of **7a** to **7b** was found by ^1H and ^{31}P NMR to be $\sim$2:1. The addition of more Cp_2MoCl_2 (1.5 equiv) yields a third Cp_2Mo(5′-dCMP) product. Attempts to separate **7a** and **7b** by chromatography on Sephadex or by fractional crystallization using a variety of anions were unsuccessful. The titration of Na_2(5′-dCMP) with Cp_2MoCl_2 in D_2O (Figure 10) reveals two new upfield nucleobase signals, two new downfield (36 ppm) phosphate signals, and two 1:1 pairs of (nonequivalent) Cp signals growing in with the incremental addition of **1**. The NMR spectral data for **7a** and **7b** (Table VIII) suggest, on the NMR time scale, nonlabile Cp_2Mo^{2+} coordination to the phosphate and a nucleobase functionality. In terms of nucleotide conformation, complex **7a**[42] shows no major changes vis-à-vis the free ligand in the sugar puckering and conformational populations along the O5′–C5′ and C5′–C4′ bonds.

The coordination of Cp_2Mo^{2+} to O3′, O2, or N4 in **7a** is unlikely since there are no significant changes in the ^1H and ^{13}C chemical shifts of H3′, C2, and N(4)H_2 and no change in the deoxyribose conformation (vide supra) upon coordination. Thus, the coordination sites in **7a** are either O(phosphate)/N3 or O(phosphate)/X (see below), where X may be a water molecule or a second O(phosphate) site on the same 5′-dCMP molecule. Only static η^2-phosphate coordination or the conformational rigidity imparted by strong intramolecular hydrogen bonding for X = H_2O[13] would afford magnetically nonequivalent Cp rings. The pH titration of **7a** (Figure 11) suggests a O(phosphate)/X coordination mode since the N3 nitrogen undergoes protonation at approximately the same pK_a (4.4)[39] as the starting Na_2(5′-dCMP). The Cp resonances in the pH titration remain magnetically nonequivalent over the entire pH. However, the O(phosphate)/N3 chelation mode cannot be completely ruled out, as it is possible that the Cp_2Mo–N3 bond in **7a** is labile under acidic conditions.

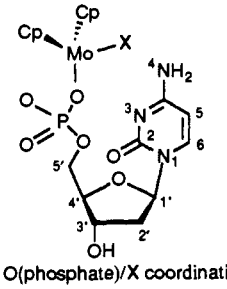

7a, O(phosphate)/X coordination

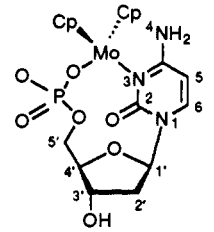

7a, O(phosphate)/N3 coordination

The ^1H NMR spectrum of **7b** in Me_2SO-d_6 reveals deprotonation of one amino proton, thus suggesting an HN4$^-$/O(phosphate) chelation mode.[43] If the crystallographically characterized

(39) Martin, B. R. *Acc. Chem. Res.* **1985**, *18*, 32–38.
(40) den Hartog, J. H. J.; van den Elst, H.; Reedijk, J. *J. Inorg. Biochem.* **1984**, *21*, 83–92.

(41) (a) Reily, M. D.; Marzilli, L. G. *J. Am. Chem. Soc.* **1986**, *108*, 8299–9300. (b) Alessio, E.; Xu, Y.; Cauci, S.; Mestroni, G.; Quadrifaglio, F.; Viglino, P.; Marzilli, L. G. *J. Am. Chem. Soc.* **1989**, *111*, 7068–7071. (c) Reily, M. D.; Hambley, T. W.; Marzilli, L. G. *J. Am. Chem. Soc.* **1988**, *110*, 2999–3007. (d) NMR data of Bose et al.[41e] on $(H_3N)_2Pt$(5′-dAMP) coordination also suggest a N7/O(phosphate) chelation mode that was proposed to involve either a dimeric or monomeric cisplatin 5′-dAMP adduct. (e) Bose, R. N.; Cornelius, R. D.; Viola, R. E. *J. Am. Chem. Soc.* **1986**, *108*, 4403–4408. (f) Green, M.; Miller, J. M. *J. Chem. Soc., Chem. Commun.* **1987**, 1864–1865. (g) Sigel, H. *ACS Symp. Ser.* **1989**, *402*, 159–204. (h) Torres, L. M.; Marzilli, L. G. *J. Am. Chem. Soc.* **1991**, *113*, 4678–4679.
(42) The coupling constants for the minor isomer could not be accurately obtained since the resonances of **7b** are partially overlapped with those of **7a**.
(43) In the pD titration of **7b**, N3 protonation cannot be observed since decomposition of both **7b** and **7a** with accompanying loss of nonequivalent Cp rings is evident below pD 3.0.

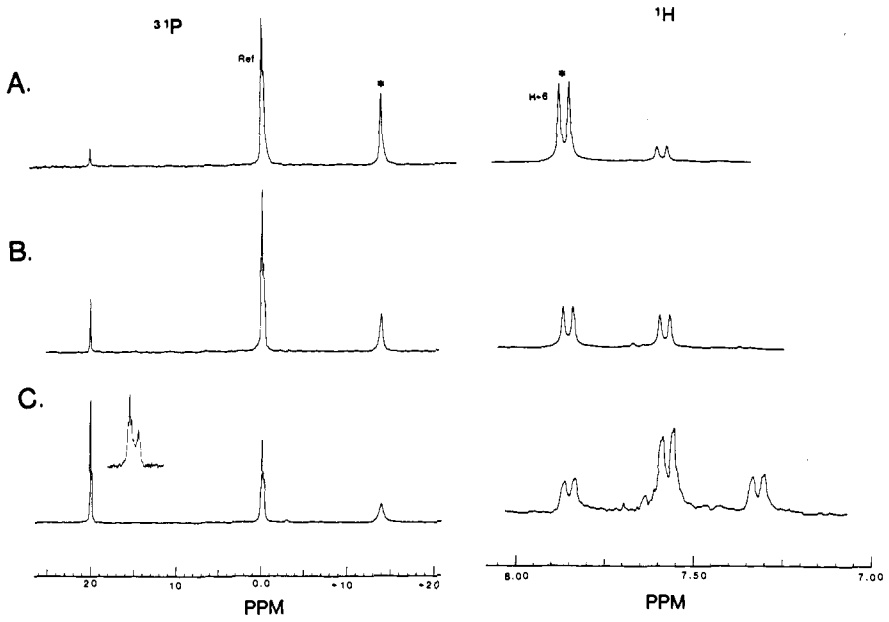

Figure 10. Titration of 2′-deoxycytidine-5′-monophosphate (5′-dCMP) with Cp_2MoCl_2 in D_2O as monitored by 270 MHz ^1H and 109 MHz ^{31}P NMR spectroscopy. Asterisks (*) represent signals of free 5′-dCMP and ref = external ^{31}P reference signal. Phosphoric acid is at −18.5 ppm relative to the ^{31}P reference: (A) 0.30 equiv of Cp_2MoCl_2, (B) 0.60 equiv of Cp_2MoCl_2, (C) 1.2 equiv of Cp_2MoCl_2. Inset in the ^{31}P spectrum shows two species (**7a** and **7b**) formed (δ 20) upon the addition of Cp_2MoCl_2.

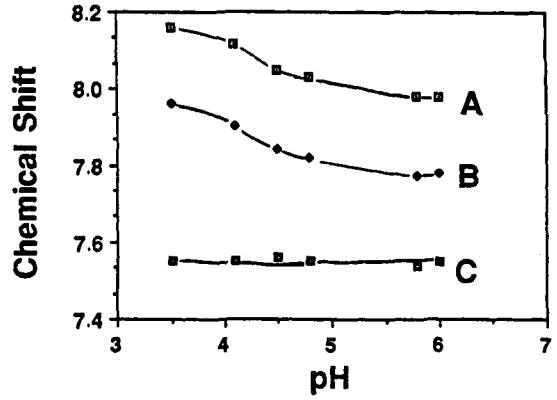

Figure 11. Chemical shift vs pH of H6 in $Cp_2Mo(5'\text{-dCMP})$ (**7a** and **7b**): (A) free 5′-dCMP, (B) product **7a**, and (C) product **7b**. The cyclopentadienyl resonances for **7a** and **7b** remain magnetically nonequivalent over the entire pH range.

$[Cp_2Mo(1\text{-methylcytosyl})][PF_6]$ complex **4** is used as a model for Mo(IV) coordination to cytosine N4, the 0.40 ppm upfield shift of the N4–H proton resonance in **7b** (Table VIII) agrees well with the 0.50 ppm upfield shift found in **4** (Table II). The aforementioned NMR spectral parameters and the pH titration results (invariant H6 chemical shift, Figure 11) thus suggest the formulation below for **7b** as the simplest model.[44] Importantly, Mo–O(phosphate) coordination is a central aspect of 5′-dCMP coordination chemistry.

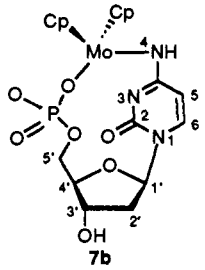

7b

(44) No molecular ion peaks corresponding to monomeric or oligomeric forms of **7b** were detected in the FAB/MS.

$Cp_2Mo(5'\text{-dTMP})$ (8). As monitored by NMR, the reaction of $Cp_2MoCl_2(aq)$ with thymidine-5′-monophosphate results in primarily one product (**8**) with accompanying minor byproducts (<5%) that could not be removed. Nevertheless, the principal $Cp_2Mo(5'\text{-dTMP})$ adduct possesses straightforwardly assigned O(phosphate)/N3 coordination (e.g., below). Thus, the observation of a 0.20 ppm upfield displacement of the nucleobase H6 resonance, a 35 ppm downfield shift of the ^{31}P signal, and magnetically nonequivalent Cp ligands (Figure 12) is reminiscent of

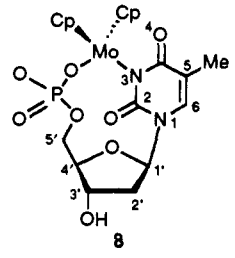

8

spectral features in $Cp_2Mo(5'\text{-dGMP})$, $Cp_2Mo(5'\text{-dAMP})$, and $Cp_2Mo(5'\text{-dCMP})$ (vide supra). Furthermore, the absence in $Me_2SO\text{-}d_6$ of the N3–H resonance (δ 11.24 in the free nucleotide) supports Mo coordination at N3. This coordination mode is further born out by the absence of IR spectral changes in the 5′-dTMP C–C and C–O double bond regions (1600–1750 cm^{-1})[45] which would be associated with carbonyl complexation. In addition, the FAB/MS spectrum exhibits a major signal at m/e 573, suggesting a monomeric $Na[Cp_2Mo(5'\text{-dTMP})]$ adduct.

Nucleotide Competition for Aqueous Cp_2MoCl_2. Solution NMR experiments were carried out to probe both $Cp_2MoCl_2(aq)$ selectivity in nucleotide binding as well as the kinetic lability of complexation (see Experimental Section for details). It was found in nucleotide competition experiments that $Cp_2MoCl_2(aq)$ exhibits little if any coordinative selectivity. Furthermore, addition of a second nucleotide to a preformed $Cp_2Mo(\text{nucleotide})$ complex in situ results in complete equilibration within the time of mixing, transporting to the NMR spectrometer, and recording a spectrum. However, ^1H NMR experiments with $Cp_2Mo(dGMP)$ + $Cp_2Mo(dTMP)$ mixtures up to +100 °C reveals no evidence of

(45) (a) Susi, H.; Ard, J. S. *Spectrochim. Acta* **1973**, *30A*, 1843–1853. (b) Lord, R. C.; Thomas, G. J. *Spectrochim. Acta* **1961**, *23A*, 2441–2591. (c) Angell, C. I. *J. Chem. Soc.* **1961**, 504–515.

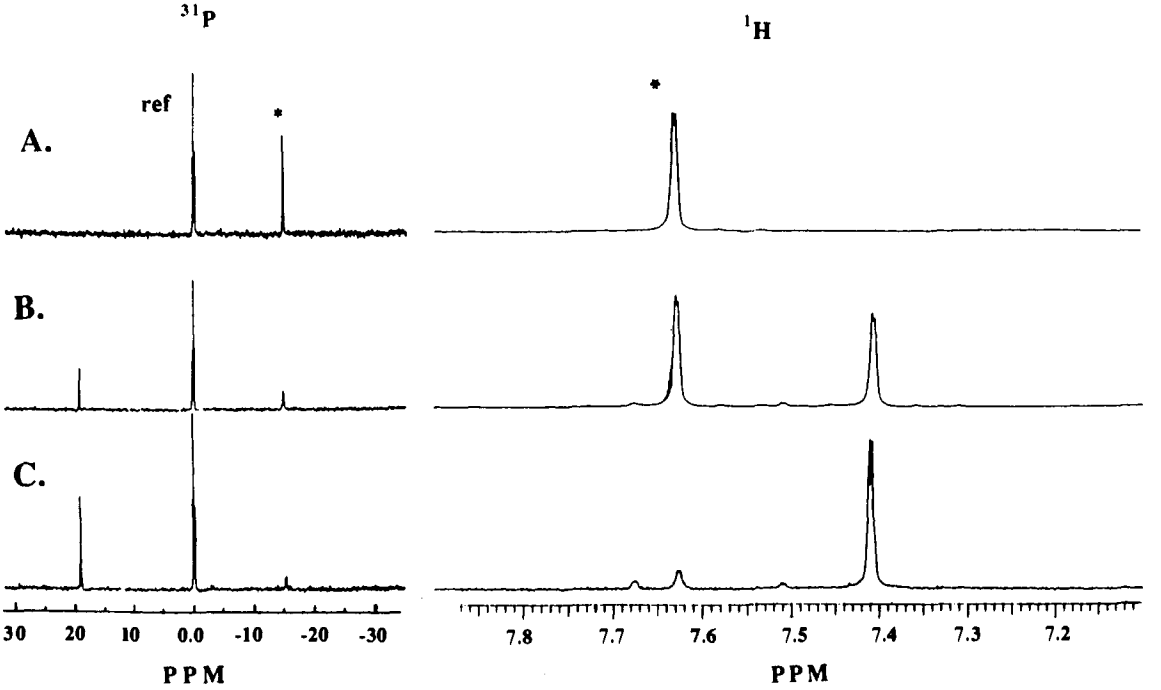

Figure 12. Titration of 2′-deoxythymidine-5′-monophosphate (5′-dTMP) with Cp_2MoCl_2 in D_2O as monitored by 400 MHz ^1H and 109 MHz ^{31}P (proton-decoupled) NMR spectroscopy. Asterisks (*) represent signals of free 5′-dTMP and ref = external ^{31}P reference signal. Phosphoric acid is at −18.5 ppm relative to the ^{31}P reference: (A) 0.0 equiv of Cp_2MoCl_2, (B) 0.50 equiv of Cp_2MoCl_2, and (C) 1.0 equiv of Cp_2MoCl_2.

Table VII. NMR Spectroscopic Data for $[Cp_2Mo(5'\text{-dGMP})]_2$ (**5**) and $Cp_2Mo(5'\text{-dAMP})$ (**6**)[a]

compound	H2[d]	H8[d]	C_5H_5[d]	N(6)H[d]	P
5′dAMP[b]	7.92 (1)	8.32 (1)			4.8
$Cp_2Mo(5'\text{-dAMP})$[b]	7.97 (1)	8.11 (1)	5.68 (5) 5.31 (5)		38.0
5′-dAMP[c]	8.12 (1)	8.44 (1)		7.30 (2)	4.8
$Cp_2Mo(5'\text{-dAMP})$[c]	8.13 (1)	8.30 (1)	5.71 (5) 5.76 (5)	7.26 (2)	42.0
5′-dGMP[b]		7.97 (1)			4.9
$Cp_2Mo(5'\text{-dGMP})$[b]		7.90 (1)	5.69 (5) 5.44 (5)		38.0

[a] ^1H chemical shift vs TMS; ^{31}P chemical shift vs 85% H_3PO_4. [b] In D_2O at pD 7.4. [c] In Me_2SO-d_6. [d] Number in parentheses denotes number of protons per formula unit by integration.

ligand exchange processes which become fast on the NMR time scale at 400 MHz. These findings are in striking contrast to the selective and kinetically nonlabile binding of cisplatin to both mononucleotides and DNA.[46]

Coordination Chemistry of a Nucleotide Methyl Ester. In order to probe possible modes of interaction of $Cp_2MoCl_2(aq)$ with the phosphodiester backbone of DNA, complexation to the methylphosphate ester of 5′-dGMP (Me(5′-dGMP), **9**) was investigated. As with $Na_2(5'\text{-dGMP})$, the titration of Me(5′-dGMP) with aqueous Cp_2MoCl_2 (pD 7.4), induces a 0.10 ppm upfield displacement of the nucleobase H8 signal and magnetically nonequivalent Cp resonances (separation ~0.010 ppm). However, there is no accompanying downfield shift in the ^{31}P signal of the phosphodiester moiety. In agreement with these ^{31}P NMR results, a titration of diphenyl phosphate ($(C_6H_5O)_2P(O)OH$) or diethyl phosphate ($(CH_3CH_2O)_2P(O)OH$) with **1** at pH 7.4 also induces no change in the ^{31}P signal. In addition, the reaction of Me(5′-dGMP) and **1** cannot be driven entirely to complete complexation of **9**, even after adding 5 equiv of **1**. Attempts to isolate Cp_2Mo^{2+} adducts of Me(5′-dGMP) by precipitation techniques, repeated crystallizations, or chromatography on Sephadex were unsuccessful. Making the reasonable assumption that Me(5′-dGMP) phosphate coordination is not accompanied by a negligible shift in the ^{31}P resonance, we conclude that *direct* Cp_2MoCl_2(aq)–phosphodiester coordination is rather weak. However, as in the case of $Cp_2VCl_2(aq)$,[13] binding to the phosphodiester via a water bridge (e.g., **10**) may be operative and could enforce magnetic nonequivalence of the Cp rings.

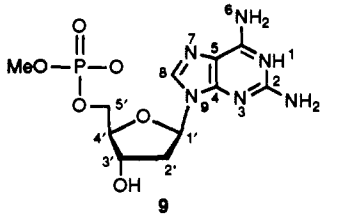

9

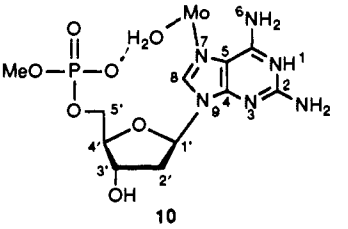

10

Effect of $Cp_2MoCl_2(aq)$ Coordination on Watson–Crick Base Pairing. In view of the destabilization of complementary nucleotide base-pairing induced by coordination of cisplatin,[47] it was of interest to determine whether $Cp_2MoCl_2(aq)$ binding effected a similar hydrogen bond alteration (this was not the case for $Cp_2VCl_2(aq)$[13]). The base pairing/hydrogen bonding between

(46) (a) Mansy, S.; Chu, G. Y. H.; Duncan, R. E.; Tobias, R. S. *J. Am. Chem. Soc.* **1978**, *100*, 607–616. (b) Fichtinger-Schepman, A. M. J.; van der Veer, J. L.; den Hartog, J. H. J.; Lohman, P. H. M.; Reedijk, J. *Biochemistry* **1985**, *24*, 707–713.

(47) (a) van Hemelryck, B.; Guittet, E.; Chottard, G.; Girault, J.-P.; Hermon, F.; Huynh-Dinh, T.; Lallemond, J.-Y.; Igolen, J.; Chottard, J.-C. *Biochem. Biophys. Res. Commun.* **1986**, *138*, 758–763. (b) den Hartog, J. H. T.; Altona, C.; van Boom, J. H.; van der Marel, G. A.; Haasnoot, C. A. G.; Reedijk, J. *J. Biomed. Struct. Dynam.* **1985**, *2*, 1137–1155. (c) Reference 34a. (d) den Hartog, J. H. T.; Altona, C.; van Boom, J. H.; van der Marel, G. A.; Haasnoot, C. A. G.; Reedijk, J. *J. Am. Chem. Soc.* **1984**, *106*, 1528–1530. (e) Lippert, B. *J. Am. Chem. Soc.* **1981**, *103*, 5691–5697. (f) Lippert, B. *Inorg. Chim. Acta* **1981**, *56*, L23–L24.

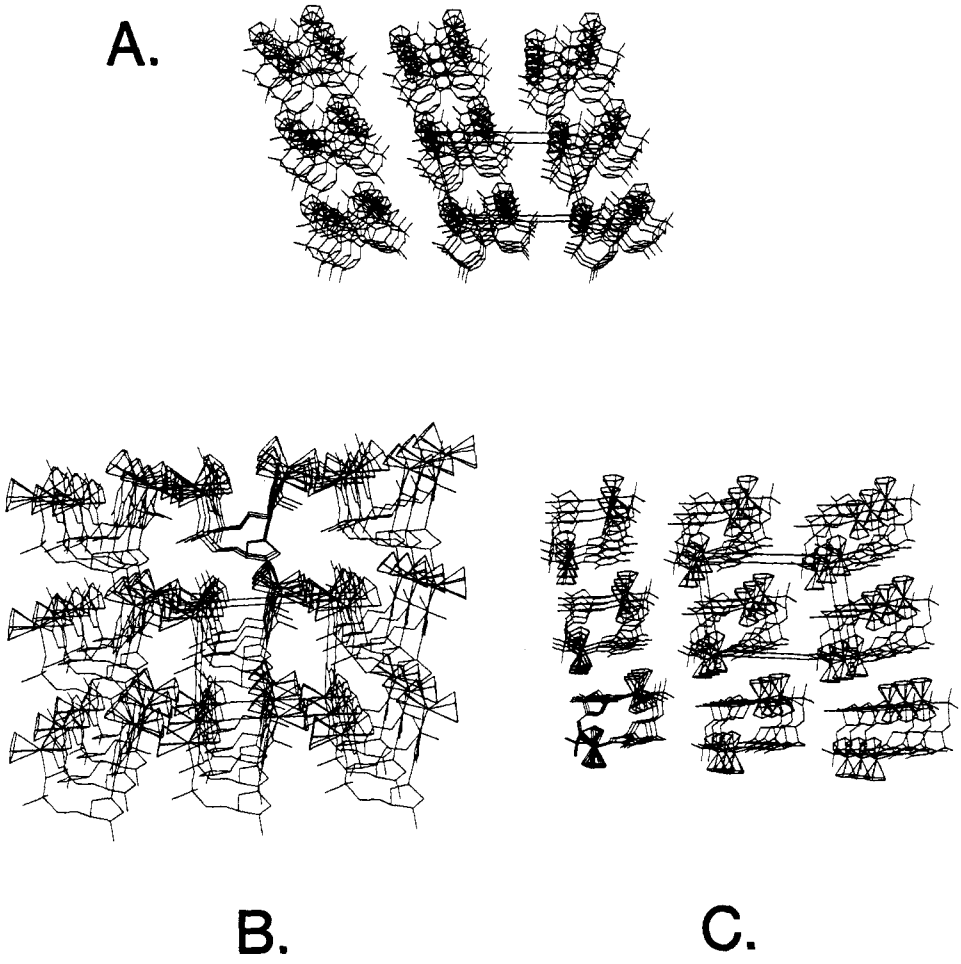

Figure 13. Unit cell packing diagram of $[Cp_2Mo(5'\text{-dGMP})]_2$ (**5**) showing the water channels extending along the (A) *a*, (B) *b*, and (C) *c* axes. Each molecule of **5** is surrounded by 13 water molecules that participate in water-bridge network extending throughout the crystal lattice.

GMP and CMP (**11**) is readily identified in the ^1H NMR at low temperature (−5.0 °C).[48] Under these conditions at pH 7.4, the

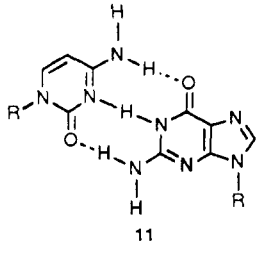

11

hydrogen-bonded amino protons of 5′-dGMP occur at δ 6.75 and 6.25, while that of 5′-dCMP occurs at δ 6.40. It is found that the addition (up to 0.5 equiv/base pair) of Cp_2MoCl_2(aq) to such a base pair solution (0.10 M) effects no major changes in the chemical shifts of the protons involved in hydrogen bonding. Major changes would be expected if the base pairing were destabilized as in the case of cisplatin.[47] Furthermore, the N4 amino resonances of 5′-dCMP remain nonequivalent upon addition of **1**, and the relative integration of these amino to H1′ proton resonances remains unchanged. This nonequivalence has been attributed to base-pairing/hydrogen-bonding interactions.[48] That Cp_2Mo^{2+} is indeed coordinated to both nucleotides is evident in the 30 ppm downfield shifts in the ^{31}P resonances, the appearance of two pairs of nonequivalent Cp resonances, and upfield shifts in the nucleobase proton signals. The ^1H and ^{31}P chemical shifts for the Cp_2Mo-coordinated 5′-dGMP/5′-dCMP base pair are within 0.05 ppm of those found in $[Cp_2Mo(5'\text{-dGMP})]_2$ (**5**) and Cp_2Mo-(5′-dCMP) (**7a**, O/X coordination).

The effect of Cp_2MoCl_2(aq) binding on the Watson–Crick base pairing between 5′-dAMP and 5′-dTMP (**12**) was studied in both water and Me_2SO-d_6.[49] The low field chemical shifts of the hydrogen-bonded 5′-dTMP N3-H and 5′-dAMP N6-H resonances are readily identified signatures of the base pairing. The addition

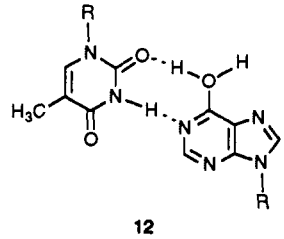

12

of **1** (0.50 equiv/base pair) to an aqueous 5′-dTMP/5′-dAMP base pair solution (−5.0 °C, pH 7.4) causes no change in the N6–H chemical shift (6.35 ppm) nor in the intensity relative to H1′ (the N3–H signals cannot be observed under these conditions). When the H_2O is removed in vacuo and replaced with Me_2SO-d_6, the chemical shift of the imino (δ 11.25) resonance also shows no change (<0.040 ppm). The characteristic ^1H and ^{31}P spectroscopic features of Cp_2MoCl_2(aq) coordination to 5′-dAMP and a ^{31}P

(48) (a) Sagan, B. L.; Walmsley, J. A. *Biochem. Biophys. Res. Commun.* **1985**, *128*, 980–986. (b) Walmsley, J. A.; Barr, R. G.; Bouhoutsos-Brown, E.; Pinnavaia, T. J. *J. Phys. Chem.* **1984**, *88*, 2599–2605. (c) Iwahashi, H.; Sugeta, H.; Kyogaku, Y. *Biochemistry* **1982**, *21*, 631–638. (d) Marzilli, L. G.; Chang, C. H.; Caradonna, J. P.; Kistenmacher, T. J. *Adv. Mol. Relax. Interact. Process* **1979**, *15*, 85–101. (e) Raszka, M.; Kaplan, N. O. *Proc. Natl. Acad. Sci. U.S.A.* **1972**, *69*, 2025–2029.

(49) The Watson–Crick base pairing between AMP and TMP is known to be stronger in Me_2SO-d_6 than in water: Saenger, W. *Principles of Nucleic Acid Structure*; Springer-Verlag: New York, 1984; pp 126–131.

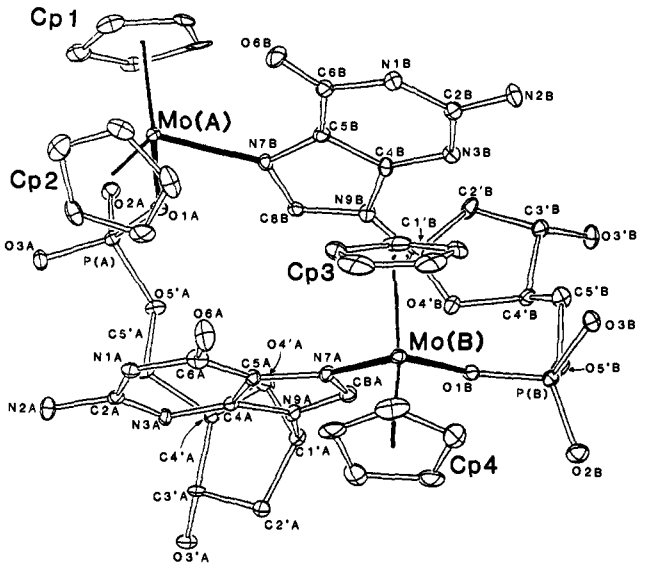

Figure 14. Perspective view of the non-hydrogen atoms of $[Cp_2Mo(5'\text{-}dGMP)]_2$ (**5**) showing the 24-membered chelate ring and dimeric molybdenum coordination. The 13 water molecules surrounding **5** are omitted for clarity. All atoms represented as thermal vibrational ellipsoids are drawn to include 30% probability. The average bond distances (Å) and angles (deg) of important metrical parameters are as follows: Mo–N7 = 2.21 (1), Mo–O1 = 2.087 (3), Mo–centroid = 1.975 (6), ∠ring centroid–Mo–ring centroid = 133.7 (5), ∠Mo–N7–C8 = 124.8 (5), ∠Mo–N7–C5 = 129.5 (4), ∠Mo–O1–P = 139.0 (9).

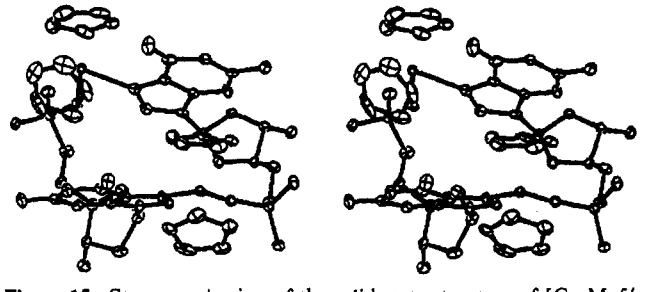

Figure 15. Stereoscopic view of the solid-state structure of $[Cp_2Mo5'\text{-}dGMP]_2$ (**5**).

downfield shift of 5′-dTMP are, however, observed (vide supra). These results argue that $Cp_2MoCl_2(aq)$ coordination has little effect on the Watson–Crick base pairing between complementary mononucleotides.

Solid-State Structure of $[Cp_2Mo(5'\text{-}dGMP)]_2$ (5). On a preparative scale, complex **5** can be obtained via the route of eq 7 (see Experimental Section for details). The X-ray structural analysis reveals that single crystals of **5** are composed of an array

$$2Cp_2MoCl_2 + 2Na_2(5'\text{-}dGMP) \xrightarrow{\text{pH 7.4}} \underset{\mathbf{5}}{[Cp_2Mo(5'\text{-}dGMP)]_2} + 4NaCl \quad (7)$$

of discrete $[Cp_2Mo(5'\text{-}dGMP)]_2$ dimers stacked as 24-membered chelate rings throughout the crystal lattice. The unit cell packing diagram in Figure 13 shows that each molecule of **5** is surrounded by water-containing channels extending along the *a*, *b*, and *c* axes. Each unit cell contains 13 water molecules (the 13th having a partial occupancy) that participate in an elaborate hydrogen-bonding network (vide infra). The Mo(IV) ion in **5** adopts the familiar "bent-sandwich" geometry found in numerous Cp_2MoX_n complexes (n = 2,[26] n = 1[27]), being π-bonded to two η^5-C_5H_5 ligands and σ-bonded to one nitrogen atom and one phosphate oxygen atom of two different mononucleotides. Final atomic coordinates for non-hydrogen atoms of **5** are presented in Table IX. Selected bond lengths, angles, and torsional angles are given in Tables X, XI, and XII, respectively. A perspective view of **5** is shown in Figure 14, and a stereoscopic presentation is given in Figure 15. Figure 16 highlights the conformational aspects of the individual 5′-dGMP ligands of **5**.

Table VIII. NMR Spectroscopic Data for $Cp_2Mo(5'\text{-}dCMP)$ (**7a** and **7b**) and $Cp_2Mo(5'\text{-}dTMP)$ (**8**)

compound	H6[d]	H5[d]	C_5H_5[d]	N(6)H[d]	P
5′-d(CMP)[b]	7.84 (1)	5.92 (1)			1.42
5′-d(CMP)[c]	7.86 (1)	5.90 (1)		7.26 (1)	1.35
				7.10 (1)	
$Cp_2Mo(5'\text{-}dCMP)$[b]					
product A	7.64 (1)	5.88 (1)	5.70 (5)		37.2
			5.65 (5)		
$Cp_2Mo(5'\text{-}dCMP)$[b]					
product B	7.40 (1)	5.34 (1)	5.74 (5)		36.5
			5.78 (5)		
$Cp_2Mo(5'\text{-}dCMP)$[c]					
product A	7.68 (1)	5.75 (1)	5.77 (5)	7.32 (1)	42.8
			5.74 (5)	7.11 (1)	
$Cp_2Mo(5'\text{-}dCMP)$[c]					
product B	7.64 (1)	5.28 (1)	5.78 (5)	6.90 (1)	42.2
			5.76 (5)		
5′-d(TMP)[b]	7.61 (1)				3.7
$Cp_2Mo(5'\text{-}dTMP)$[b]	7.39 (1)		5.74 (5)		37.8
			5.69 (5)		

[a] ^1H data vs TMS; ^{31}P data vs 85% H_3PO_4. [b] In D_2O at pD 7.4. [c] In Me_2SO-d_6. [d] Number in parentheses denotes number of protons per formula unit by integration.

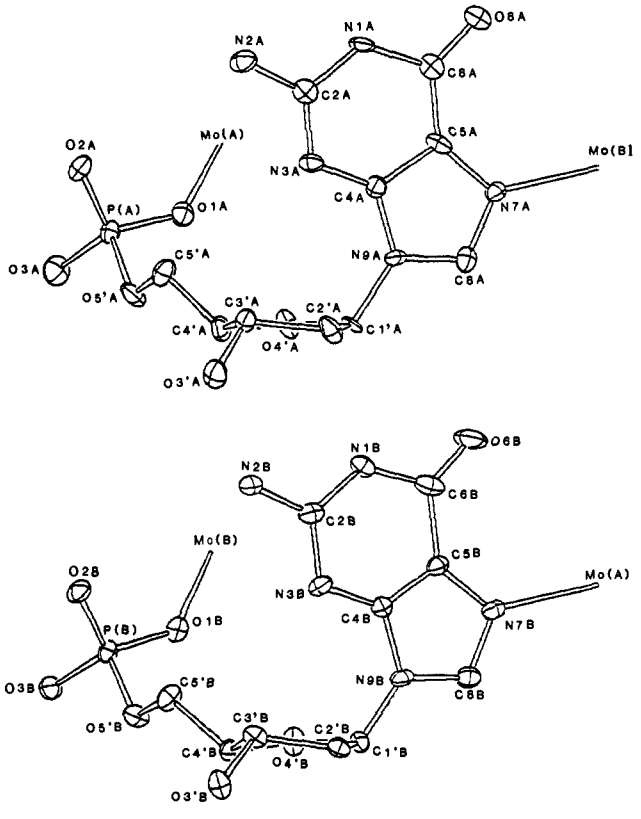

Figure 16. Perspective view of both deoxyribonucleotide moieties in **5** showing the syn, β^{gg}, γ^{gt}, and C3′-endo nucleotide conformations. Important torsional angles (deg) are as follows: P–O5′–C5′–C4′ (av) = 146.2 (5), O5′–C5′–C4′–C3′ (av) = 168 (1), C5′A–C4′A–C3′A–O3′A = 97.7 (7), C5′B–C4′B–C3′B–O3′B = 105.5 (7), and O4′–C1′–N9–C4 (av) = 65.0 (8).

A pseudoinversion center in the 24-membered chelate ring of **5** (Figure 14) relates the two "outside" cyclopentadienyl ligands, Cp1 and Cp4, as well as the "inside" cyclopentadienyl ligands, Cp2 and Cp3. These crystallographic results for the cyclopentadienyl environment are consistent with the aforementioned NMR spectroscopic results that show two magnetically nonequivalent Cp environments. As in compounds **3a** and **4**, the Cp_2Mo ligation in **5** is metrically unexceptional. The average C–C distance (1.41 (1) Å), Mo–C distance (2.31 (1) Å), and Mo–

Table X. Selected Bond Lengths (Å)[a] for Cp_2Mo(2′-deoxyguanosine-5′-monophosphate) (**5**)

atom 1	atom 2	distance (Å)	atom 1	atom 2	distance (Å)
Mo(A)	O1A	2.083 (5)	Mo(B)	O1B	2.090 (5)
Mo(A)	N7B	2.193 (6)	Mo(B)	N7A	2.221 (6)
Mo(A)	C(11)	2.336 (8)	Mo(B)	C(31)	2.31 (1)
Mo(A)	C(12)	2.36 (1)	Mo(B)	C(32)	2.365 (9)
Mo(A)	C(13)	2.315 (9)	Mo(B)	C(33)	2.29 (1)
Mo(A)	C(14)	2.230 (8)	Mo(B)	C(34)	2.26 (1)
Mo(A)	C(15)	2.279 (8)	Mo(B)	C(35)	2.311 (9)
Mo(A)	Cg1	1.972	Mo(B)	Cg3	1.976
Mo(A)	C(21)	2.261 (8)	Mo(B)	C(41)	2.32 (1)
Mo(A)	C(22)	2.262 (9)	Mo(B)	C(42)	2.31 (1)
Mo(A)	C(23)	2.33 (1)	Mo(B)	C(43)	2.231 (8)
Mo(A)	C(24)	2.393 (9)	Mo(B)	C(44)	2.307 (8)
Mo(A)	C(25)	2.322 (8)	Mo(B)	C(45)	2.341 (8)
Mo(A)	Cg2	1.968	Mo(B)	Cg4	1.981
C(11)	C(12)	1.44 (1)	C(31)	C(32)	1.41 (1)
C(12)	C(13)	1.37 (1)	C(32)	C(33)	1.45 (2)
C(13)	C(14)	1.43 (1)	C(33)	C(34)	1.43 (2)
C(14)	C(15)	1.43 (1)	C(34)	C(35)	1.39 (2)
C(15)	C(11)	1.41 (1)	C(35)	C(31)	1.41 (2)
C(21)	C(22)	1.41 (1)	C(41)	C(42)	1.35 (2)
C(22)	C(23)	1.46 (1)	C(42)	C(43)	1.39 (1)
C(23)	C(24)	1.41 (1)	C(43)	C(44)	1.44 (1)
C(24)	C(25)	1.44 (2)	C(44)	C(45)	1.38 (2)
C(25)	C(21)	1.40 (1)	C(45)	C(41)	1.39 (2)
P(A)	O2A	1.504 (5)	P(B)	O2B	1.500 (5)
P(A)	O3A	1.516 (5)	P(B)	O3B	1.512 (6)
P(A)	O1A	1.539 (5)	P(B)	O1B	1.540 (5)
P(A)	O5′A	1.609 (5)	P(B)	O5′B	1.605 (6)
N7A	C8A	1.315 (9)	N7B	C8A	1.327 (9)
C8A	N9A	1.372 (9)	C8B	N9B	1.362 (8)
N9A	C4A	1.373 (8)	N9B	C4B	1.375 (9)
N9A	C1′A	1.458 (8)	N9B	C1′B	1.475 (8)
C4A	C5A	1.38 (1)	C4B	C5B	1.41 (1)
C5A	N7A	1.403 (9)	C5B	N7B	1.416 (9)
C5A	C6A	1.44 (1)	C5B	C6B	1.41 (1)
C6A	O6A	1.23 (1)	C6B	O6B	1.22 (1)
C6A	N1A	1.41 (1)	C6B	N1B	1.39 (1)
N1A	C2A	1.36 (1)	N1B	C2B	1.37 (1)
C2A	N2A	1.36 (1)	C2B	N2B	1.37 (1)
C2A	N3A	1.327 (9)	C2B	N3B	1.33 (1)
C1′A	C2′A	1.53 (1)	C1′B	C2′B	1.53 (1)
C2′A	C3′A	1.52 (1)	C2′B	C3′B	1.54 (1)
C3′A	O3′A	1.434 (8)	C3′B	O3′B	1.414 (9)
C3′A	C4′A	1.53 (1)	C3′B	C4′B	1.53 (1)
C4′A	O4′A	1.447 (8)	C4B	O4′B	1.46 (1)
O4′A	C1′A	1.426 (8)	O4′B	C1′B	1.417 (9)
C4′A	C5′A	1.51 (1)	C4′B	C5′B	1.51 (1)
C5′A	O5′A	1.426 (8)	C5′B	O5′B	1.424 (9)

[a] Estimated standard deviations in the least significant figure are given in parentheses. Cg1, Cg2, Cg3, and Cg4 are the centroids of the rings composed of atoms C(11)–C(15), C(21)–C(25), C(31)–C(35), and C(41)–C(45), respectively.

centroid distance (Mo–Cg = 1.98 (1) Å) compare favorably with the corresponding bond distances in **3a**, **4**, and Cp_2MoCl_2.[26f] The Cg–Mo–Cg angles (134.4° and 133.2°) in **5** are close to corresponding angles found in **3a** and **4**. The two Mo–N7 distances (2.18 (1) and 2.22 (1) Å) can be compared with Mo(IV)–N bond distances that range from 2.188 (6) to 2.256 (7) Å in other Cp_2MoX_n[26,27] complexes, including **3a** and **4** (vide supra). The two Mo–O(phosphate) distances (2.093 (8) and 2.099 (9) Å) are close to the average Mo–O(phosphate) distance of 2.126 (9) Å in $[Cp_2MoO_2PO_2MoCp_2]PF_6$[27e] and can be compared with Mo–O bond distances of 2.078 (7) Å in $[Cp_2Mo(\text{L-leucine})][PF_6]$ ($Cp_2Mo(H_2NC_5H_{12}COO)$),[27d] 2.108 (4) Å in $[Cp_2Mo(\text{L-proline})][PF_6]$ ($Cp_2Mo(NHC_4H_8COO)$),[27d] and 2.113 (4) in $Cp_2Mo(SO_4)$.[27b]

5′-dGMP Conformation in $[Cp_2Mo(dGMP)]_2$. It is evident that Cp_2Mo^{2+} binding to 5′-dGMP results in major conformational changes in the 5′-dGMP molecule. Both 5′-dGMP nucleotide fragments of **5** (Figure 16), which are in the C3′-endo sugar and syn glycosidic conformation, undergo only minor metrical changes

Table XI. Selected Bond Angles[a] for Cp_2Mo(2′-deoxyguanosine-5′-monophosphate) (**5**)

atom 1	atom 2	atom 3	angle (deg)	atom 1	atom 2	atom 3	angle (deg)
O1A	Mo(A)	N7B	77.5 (2)	O1B	Mo(B)	N7A	78.0 (2)
O1A	Mo(A)	Cg1	109.54	O1B	Mo(B)	Cg3	109.16
O1A	Mo(A)	Cg2	106.36	O1B	Mo(B)	Cg4	108.63
N7B	Mo(A)	Cg1	108.01	N7A	Mo(B)	Cg3	108.8
N7B	Mo(A)	Cg2	106.54	N7A	Mo(B)	Cg4	105.09
Cg1	Mo(A)	Cg2	134.35	Cg3	Mo(B)	Cg4	133.22
C(11)	C(12)	C(13)	108.5 (8)	C(31)	C(32)	C(33)	106.1 (9)
C(12)	C(13)	C(14)	108.7 (8)	C(32)	C(33)	C(34)	106.2 (8)
C(13)	C(14)	C(15)	107.2 (8)	C(33)	C(34)	C(35)	110 (1)
C(14)	C(15)	C(11)	107.7 (8)	C(34)	C(35)	C(11)	107 (1)
C(15)	C(11)	C(12)	107.8 (8)	C(35)	C(31)	C(32)	111 (1)
C(21)	C(22)	C(23)	108.3 (9)	C(41)	C(42)	C(43)	107 (1)
C(22)	C(23)	C(24)	106.6 (9)	C(42)	C(43)	C(44)	108.6 (9)
C(23)	C(24)	C(25)	108.3 (8)	C(43)	C(44)	C(45)	105.3 (8)
C(24)	C(25)	C(21)	108.4 (8)	C(44)	C(45)	C(41)	109 (1)
C(25)	C(21)	C(22)	108.4 (9)	C(45)	C(41)	C(42)	110 (1)
Mo(A)	O1A	P(A)	139.8 (3)	Mo(B)	O1B	P(B)	138.1 (3)
O1A	P(A)	O5′A	103.8 (3)	O1B	P(B)	O5′B	103.2 (3)
O1A	P(A)	O2A	112.3 (3)	O1B	P(B)	O2B	113.2 (3)
O1A	P(A)	O3A	112.4 (3)	O1B	P(B)	O3B	111.9 (3)
O2A	P(A)	O3A	113.7 (3)	O2B	P(B)	O3B	115.0 (3)
O2A	P(A)	O5′A	109.5 (3)	O2B	P(B)	O5′A	108.8 (3)
O3A	P(A)	O5′A	104.3 (3)	O3B	P(B)	O5′B	103.5 (3)
P(A)	P5′A	C5′A	118.1 (4)	P(B)	O5′B	C5′B	119.0 (5)
O5′A	C5′A	C4′A	111.8 (6)	O5′B	C5′B	C4′B	109.9 (6)
C5′A	C4′A	C3′A	110.7 (6)	C5′B	C4′B	C3′B	113.0 (6)
C4′A	C3′A	O3′A	110.6 (6)	C4′B	C3′B	O3′B	113.0 (6)
C5′A	C4′A	O4′A	110.2 (6)	C5′B	C4′B	O4′B	109.1 (6)
C4′A	C3′A	C2′A	105.1 (6)	C4′B	C3′B	C2′B	105.1 (6)
O3′A	C3′A	C2′A	112.2 (6)	O3′B	C3′B	C2′B	109.2 (6)
C3′A	C2′A	C1′A	105.2 (6)	C3′B	C2′B	C1′B	105.2 (6)
C2′A	C1′A	O4′A	107.8 (5)	C2′B	C1′B	O4′B	109.7 (6)
C2′A	C1′A	N94	114.6 (6)	C2′B	C1′B	N9B	111.8 (6)
C1′A	O4′A	C4′A	110.9 (5)	C1′B	O4′B	C4′B	110.1 (5)
O4′A	C1′A	N9A	107.8 (5)	C4′B	C1′B	N9B	109.0 (5)
O4′A	C4′A	C3′A	106.5 (6)	O4′B	C4′B	C3′B	107.8 (6)
C1′A	N9A	C8A	126.1 (6)	C1′B	N9B	C8B	124.3 (6)
C1′A	N9A	C4A	126.7 (6)	C1′B	N9B	C4B	126.7 (5)
N9A	C4A	C5A	106.0 (6)	N9B	C4B	C5B	105.4 (6)
N9A	C4A	N3A	125.1 (6)	N9B	C4B	N3B	126.3 (6)
C4A	N3A	C2A	113.0 (6)	C4B	N3B	C2B	113.4 (6)
C4A	C5A	N7A	109.5 (6)	C4B	C5B	N7B	108.6 (6)
N3A	C2A	N2A	118.7 (7)	N3B	C2B	N2B	119.2 (7)
N3A	C2A	N1A	123.0 (6)	N3B	C2B	N1B	122.0 (7)
N2A	C2A	N1A	118.3 (6)	N2B	C2B	N1B	118.8 (7)
C2A	N1A	C6A	125.9 (6)	C2B	N1B	C6B	126.5 (6)
N1A	C6A	O6A	119.8 (7)	N1B	C6B	O6B	118.7 (7)
O6A	C6A	C5A	129.0 (8)	O6B	C6B	C5B	129.2 (7)
N1A	C6A	C5A	111.1 (6)	N1B	C6B	C5B	112.2 (6)
C6A	C5A	C4A	118.0 (6)	C6B	C5B	C4B	117.6 (7)
C6A	C5A	N7A	132.5 (7)	C6B	C5B	N7B	133.8 (7)
C5A	C4A	N3A	128.9 (6)	C5B	C4B	N3B	128.3 (6)
C5A	N7A	C8A	105.2 (6)	C5B	N7B	C8B	105.6 (5)
C5A	N7A	Mo(B)	129.9 (4)	C5B	N7B	Mo(A)	129.1 (4)
N7A	C8A	N9A	112.1 (6)	N7B	C8B	N9B	111.7 (6)
C8A	N9A	C4A	107.1 (5)	C8B	N9B	C4B	108.6 (5)
C8A	N7A	Mo(B)	124.3 (5)	C8B	N7B	Mo(A)	125.3 (4)

[a] Estimated standard deviations in the least significant figure are given in parentheses. See note *a* in Table XIV for definitions of Cg1–Cg4.

when coordinated. Cp_2Mo^{2+} coordination does not alter the O–P–O bond angles in **5** relative to the starting Na_2(5′-dGMP).[50] The equal P–O2 and P–O3 bond lengths suggest a delocalized negative charge between O2 and O3. Finally, the C5–N7–C8 bond angle as well as the C5–N7 and N7–C8 bond lengths are also unaltered by Cp_2Mo^{2+} coordination.

The crystal structure of **5** reveals that the glycosidic conformation about C1′–N9 is in the "high syn" range,[51] in contrast to the "anti" conformation found in the starting Na_2(5′-dGMP).[50] The conformation about the O5′–C5′ bond in **5** is in the

(50) (a) Young, D. W.; Tollin, P.; Wilson, H. R. *Nature* **1974**, *248*, 513–514. (b) Young, D. W.; Tollin, P.; Wilson, H. R. *Acta Cryst. B* **1974**, *30*, 2012–2128. (c) Viswamitra, M. A.; Seshadri, T. P. *Nature* **1974**, *252*, 176–177.

(51) Reference 49, pp 9–28.

Table XII. Selected Torsional Angles[a] and Pseudorotation Angles (P)[b] (deg) for $Cp_2Mo(2'$-deoxyguanosine-$5'$-monophosphate) (**5**) and Disodium $2'$-Deoxyguanosine-$5'$-monophosphate ($Na_2(5'$-dGMP))

torsional angle	molecule A	molecule B	$Na_2(5'$-dGMP)[c]
χ	64.2 (8)	65.9 (8)	236.9
β	−146.7 (5)	−145.7 (5)	112.8
γ	−169.5 (7)	−167.0 (8)	175.4
δ	97.7 (7)	105.5 (7)	93.4
ν_0	−3.8 (7)	−1.7 (7)	−37.9
ν_1	−9.8 (7)	−7.6 (8)	19.4
ν_2	18.7 (7)	13.4 (7)	4.4
ν_3	−21.2 (7)	−14.8 (8)	−26.5
ν_4	15.8 (7)	10.6 (8)	40.3
P	28	25	84

[a] Torsional angles β, γ, δ, and χ are defined in refs 49, Chapter 2, and 52b. The ribose torsional angles ν_0–ν_4 are defined in refs 49, Chapter 2, and 52b. [b] Pseudorotation phase angles are calculated from the ribose torsional angles as described in ref 52. [c] Torsional angles for $Na_2(5'$-dGMP) are taken from ref 50.

Table XIII. Intermolecular Bond Distances (Å) and Angles (deg) in $[Cp_2Mo(5'$-dGMP)$]_2$ (**5**) and Water Contact Distances

Possible Hydrogen Bonding Modes

atom 1	atom 1	distance	atom 1	atom 2	distance
O2A[a]	O(W4)	2.79 (1)	O(W4)	O3B[b]	2.735 (9)
O3A[c]	O(W11)	2.774 (8)	O(W11)	O3B	2.807 (8)
O2A[b]	O(W12)	2.76 (1)	O(W12)	N2B	2.80 (1)
O2B	O(W5)	2.687 (8)	O(W5)	N2A[d]	2.94 (1)
			O(W5)	O3′A[h]	2.780 (8)
O2A	O(W13)	2.710 (4)	O(W13)	O3′B	2.69 (1)
O2B[e]	O(W1)	2.635 (8)	O(W1)	O3′A	2.833 (8)

atom 1	atom 2	atom 3	angle
O2A	O(W4)	O3B	116.3 (3)
O3A	O(W11)	O3B	118.6 (3)
O2A	O(W12)	N2B	118.1 (3)
O2B	O(W5)	N2A	105.2 (3)
O2B	O(W5)	O3′A	98.4 (3)
O2A	O(W13)	O3′B	105.9 (3)
O2B	O(W1)	O3′A	98.3 (2)

Water Contact Distances

atom 1	atom 2	distance	atom 1	atom 2	distance
O2A[f]	O(W2)	2.657 (9)	O3B[b]	O(W3)	2.67 (1)
N2A[d]	O(W6)	2.91 (1)	O6A[g]	O(W7)	2.91 (1)
O3A[h]	O(W8)	2.774 (8)	N2B	O(W9)	2.804 (9)

[a] Intermolecular lattice translations: $x+1, y, z$. [b] $x, y+1, z$. [c] $x-1, y+1, z$. [d] $x, y-1, z$. [e] $x, y+1, z+1$. [f] $x+1, y, z$. [g] $x+1, y, z+1$. [h] $x, y-1, z-1$.

gauche–gauche range[51] and the P–O5′–C5′–C4′ torsional angles in **5** show a 100° change from the corresponding angle in $Na_2(5'$-dGMP) (Table XII).[50] On the other hand, the O5′–C5′–C4′–C3′ and C5′–C4′–C3′–O4′ torsional angles in **5** are comparable to those found in $Na_2(5'$-dGMP)[50] (Table XII) and fall within the gauche–trans and trans–gauche classification,[51] respectively. The sugar conformation of the two deoxyribose rings in **5** is described by the pseudorotation phase angle, P, which is calculated from the deoxyribose torsional angles.[52] The pseudorotation phase angle for deoxyribonucleotides is generally found to fall within two ranges: $0° \le P \le 36°$ (C3′-endo) and $144° \le P \le 190°$ (C2′-endo).[52] Thus the two pseudorotation angles for **5**, $P_A = 28°$ and $P_B = 25°$, reveal both deoxyribose rings to be in the C3′-endo puckering geometry as shown additionally in Figure 16.

The solution NMR spectroscopic results for **5** (vide supra) are in generally good agreement with solid-state crystallographic data.

(52) (a) The pseudorotation angle, P, is defined as $\tan P = [(V_4 + V_1) - (V_3 + V_0)]/2V_2(\sin 36° + \sin 72°)$ where the four deoxyribose torsional angles V_0, V_1, V_2, V_3, V_4 refer to atom groups C4′–O4′–C1′–C2′, O4′–C1′–C2′–C3′, C1′–C2′–C3′–C4′, C2′–C3′–C4′–O4′, and C3′–C4′–O4′–C1′, respectively. (b) Altona, C.; Sundaralingam, M. *J. Am. Chem. Soc.* **1972**, *94*, 8205–8212.

Table XIV. pK_a Data for Water Molecules Bound to *cis*-$Pt(NH_3)_2(H_2O)_2^{2+}$ and $Cp_2M(H_2O)_2^{2+}$ Complexes

complex	pK_{a1}	pK_{a2}
cis-$Pt(NH_3)_2(H_2O)_2^{2+}$[a]	5.6	7.3
$Cp_2Ti(H_2O)_2^{2+}$[b,c]	3.51 (5)	4.35 (9)
$Cp_2V(H_2O)_2^{2+}$[b,c]	4.73 (3)	5.15 (13)
$Cp_2Mo(H_2O)_2^{2+}$[b]	5.5 (3)	8.5 (3)

[a] At 20 °C: Jensen, K. A. *Z. Anorg. Allg. Chem.* **1939**, *242*, 87–91. [b] At 37 °C: 0.318 M KNO_3. [c] Reference 12.

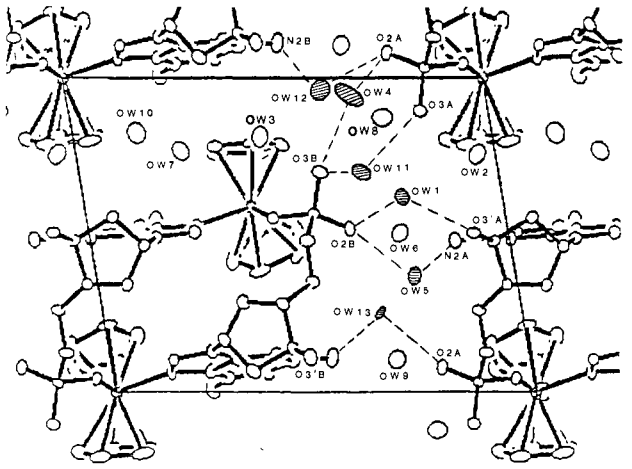

Figure 17. View of the $[Cp_2Mo(5'$-dGMP$)]_2$ crystal structure viewed down the c axis with water molecules included. Water molecules bridging the individual $[Cp_2Mo(5'$-dGMP$)]_2$ units, O(W12), O(W11), O(W1), O(W5), and O(W13) are highlighted, and the probable hydrogen bonds are represented by dashed lines.

Both techniques show that the conformation about the O5′–C5′ bond lies toward the gauche–gauche classification and that the nucleobase H8 proton is in close proximity to H1′ and H2′. In connection with the sugar puckering and the C5′–C4′ rotamer, the NMR data show an equilibrium mixture of the possible ribose puckering modes, and a preference for the gauche–gauche conformation along the C5′–C4′ bond while the crystallographic results show that both 5′-dGMP nucleotides are in C3′-endo and gauche–trans conformation. Molecular models of **5** reveal that there is sufficient conformational flexibility in the 5′-dGMP molecule such that the differences in the solution and solid-state conformations represent only minor torsional changes about the deoxyribose bonds.

Hydrogen Bond Interactions in $[Cp_2Mo(dGMP)]_2$. The unit cell packing diagram in Figure 13 shows that each dimeric unit of **5** is surrounded by water-containing channels extending along the a, b, and c axes. In addition, there is evidence for possible intermolecular hydrogen bonds as certain water oxygen atoms (O(W)) readily bridge the N2, O3′, and phosphate oxygen atoms of different molecules of **5**. In determining the possible hydrogen bond interactions, intermolecular contact distances less than 3.0 Å were chosen. Metrical details for the possible hydrogen bonds between individual $[Cp_2Mo(5'$-dGMP$)]_2$ molecules are set out in Table XIII and drawn in Figure 17. It can be seen that the water oxygen atoms, O(W12), O(W4), O(W11), O(W1), O(W5), and O(W13) are well suited to serve as intermolecular water bridges with average O(W)–O and O(W)–N contact distances of 2.77 (9) Å, indicating a weak hydrogen bond.[53] Furthermore, the angles at the water oxygen atoms varying from 98° to 120° are in the range of hydrogen bond interactions.[53] The remaining water molecules are clustered around the phosphate oxygen and amino nitrogen atoms (av O(W)···O and O(W)···N = 2.70 (9) Å) and do not exhibit distances and angles that indicate hydrogen-bonding interactions with **5**.

(53) (a) Novak, A. *Struct. Bonding* **1974**, *18*, 177–216. (b) Hamilton, W. C.; Ibers, J. A. *Hydrogen Bonding in Solids*; W. A. Benjamin, Inc: New York, 1968; pp 161–237.

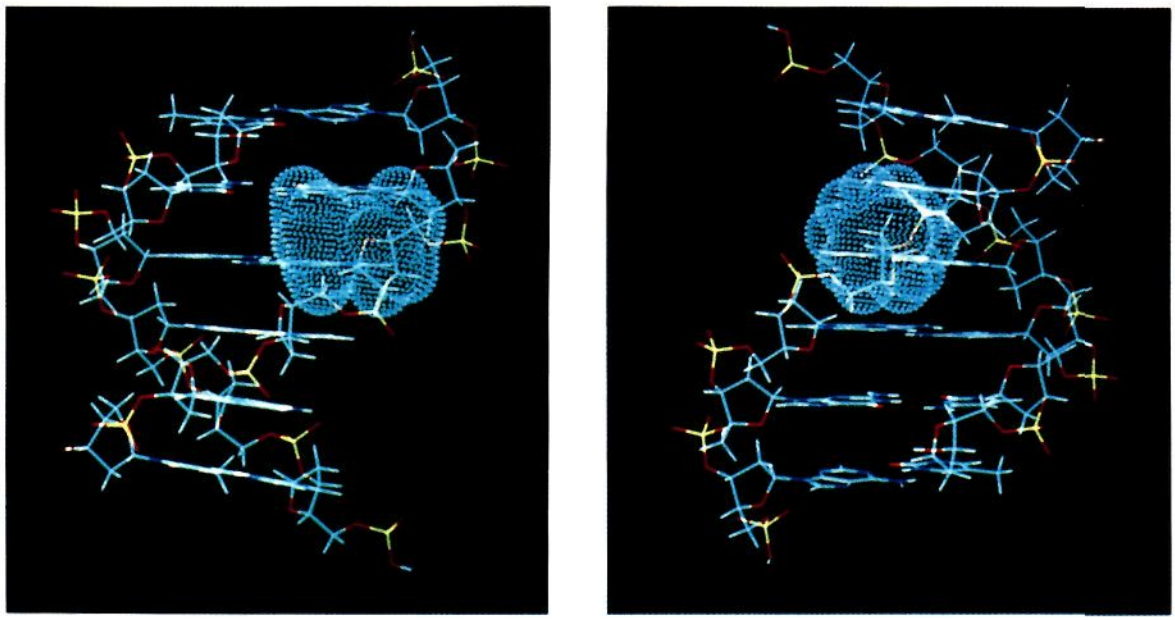

Figure 18. Molecular graphics depiction of the docking of Cp_2Mo^{2+} to the N7 positions of two adjacent guanine bases of the energy-minimized, self-complementary hexamer duplex $[d(pApGpGpCpCpT)]_2$. Key: light blue, carbon atoms; red, oxygen atoms; dark blue, nitrogen atoms; yellow, phosphorus atoms; white, hydrogen atoms. The van der Waals surfaces of the Cp_2Mo^{2+} unit appear in blue, with the Cg–Mo–Cg plane oriented perpendicular to the helix axis: (A, left) view with the metallocene "wedge" opening away from the viewer and (B, right) ensemble of Figure 18A rotated 90° about the helix axis. The Cg–Cg axis is perpendicular to the plane of the page with the metallocene "wedge" opening to the right.

Discussion

This study provides the most detailed solution and solid-state structural picture to date of the modes by which antineoplastic $Cp_2MX_2(aq)$ species can coordinate to DNA constituents under conditions approximating physiological. Furthermore, the information garnered on the "softer" metal center in Cp_2MoCl_2 complements previous results obtained on Cp_2TiCl_2, Cp_2ZrCl_2, and Cp_2VCl_2.[12,13]

Aqueous Chemistry of Cp_2MoCl_2. In regard to hydrolytic stability of the M–Cp linkage, the inertness of **1** most closely parallels that of Cp_2VCl_2 and stands in contrast to the facile ring loss of Cp_2TiCl_2 and Cp_2ZrCl_2. The reason is probably a combination of smaller metal ion size, better metal-ring orbital overlap/softness, and greater electronic population of metal-ring bonding orbitals. However, of the Cp_2MCl_2 complexes studied to date, Cp_2MoCl_2 exhibits the most rapid and extensive chloride hydrolysis. The rapid chloride dissociation goes to completion after an hour in unbuffered pH solution and instantaneously reaches $[Cl^-]/[M] = 2.0$ when the pH is brought to neutrality. This property is not readily rationalized on the basis of ion size or orbital overlap and may instead reflect electronic population of Mo–Cl orbitals with significant antibonding character. In any case, the present enhanced chloride lability represents a greater Cp_2MCl_2 departure from the properties of cisplatin than observed for M = Ti, V.

The product of Cp_2MoCl_2 aquation is proposed to be a hydroxoaquo species such as $Cp_2Mo(H_2O)OH^+$ (cf. eqs 1–4). The pK_a values of the bound water molecules are found to be rather high, and as can be seen in Table XIV, $Cp_2M(H_2O)_2^{2+}$ acidity declines as M becomes more electron-rich. In contrast to Cp_2VCl_2 and cisplatin, which exist predominantly as neutrally charged $Cp_2V(OH)_2$ and $(NH_3)_2PtCl_2$ at physiological (serum) pH and Cl^- concentration, Cp_2MoCl_2 exists as a *cationic* species. The charged nature of $Cp_2MoCl_2(aq)$ may rationalize the somewhat lower cytoxicity of Cp_2MoCl_2 against HEp-2 carcinoma in vitro[3b] and the lower in vitro metal accumulation by TA3Ha cells vis-à-vis cisplatin and Cp_2VCl_2.[3b]

Cp_2Mo^{2+} Coordination to Nucleobases. The chelation mode in **3a** and **4** models the binding of Cp_2Mo^{2+} to nucleobases and serves as the basis for understanding the coordination of $Cp_2MoCl_2(aq)$ to 2′-deoxymononucleotides. The metal coordination in both complexes **3a** and **4** involves an apparently strained, four-membered Mo(IV) chelate ring, deprotonation of one amino proton, and simultaneous coordination to both the endo- and exocyclic nitrogen atoms of the nucleobase. For pyrimidine bases, metals typically coordinate to the endocyclic N3 or O2 atoms, and unless deprotonated in strongly basic solutions, exocyclic amino groups are usually not metal binding sites.[54,55] Likewise, for purine nucleobases, endocyclic N7 is the preferred site for metal binding. Indeed, our ^1H NMR studies suggest NH(6)/N7 chelation to the 9-methyladenine ligand for **3b** while the **3a** isomer involves NH(6)/N1 chelation. To our knowledge, the only other examples of metal coordination to *both* N1 and N7 of 9-methyladenine are the polymeric crystal structures of (μ-9-methyladenine)silver(I) nitrate,[57] and dichloro(μ-9-methyladenine)cobalt(II),[58] both of which contain a cationic chain with each metal ion bonded to N7 and N1 of different 9-methyladenyl ligands. In addition crystallographically characterized examples of N1 coordination involving 9-methyladenine are known for zinc,[59a] platinum,[59b] and mercury[59c] complexes.

The crystal structure of *trans,trans*-$[Pt(NH_3)_2(1\text{-methylcytosyl})_2](NO_3)_2\cdot 2H_2O$[60] reveals strong parallels to **3a** and **4** in

(54) (a) Barton, J. K.; Lippard, S. J. In *Nucleic Acid–Metal Interactions*; Spiro, T. G., Ed.; Wiley: New York, 1980; pp 32–113. (b) Marzilli, L. G. *Prog. Inorg. Chem.* Lippard, S. J., Ed.; **1982**, *23*, 256–367.

(55) (a) Faggiani, R.; Lippert, B.; Lock, C. J. L.; Speranzini, R. A. *J. Am. Chem. Soc.* **1981**, *103*, 1111–1120. (b) Faggiani, R.; Lippert, B.; Lock, C. J. L.; Sperazini, R. A. *J. Am. Chem. Soc.* **1981**, *103*, 1111–1120. (c) Aoki, K. *J. Am. Chem. Soc.* **1981**, *20*, 335–338. (d) Graves, B. J.; Hodgson, D. J. *J. Am. Chem. Soc.* **1979**, *101*, 5608–5612. (e) Clarke, M. J. *J. Am. Chem. Soc.* **1978**, *100*, 50068–5075. (f) Sinn, E.; Flynn, C. M.; Martin, R. B. *Inorg. Chem.* **1977**, *16*, 2403–2406.

(56) (a) Sheldrick, W. S.; Bell, P. *Inorg. Chim. Acta* **1986**, *123*, 181–187. (b) Beyerle-Pfnur, R.; Brown, B.; Faggiani, R.; Lippert, B.; Lock, C. J. L. *Inorg. Chem.* **1985**, *24*, 4001–4009. (c) Charland, J.-P.; Beauchamp, A. L. *Croat. Chem. Acta* **1984**, *57*, 679–687. (d) Kistenmacher, T. J.; Marzilli, L. G.; Szalda, D. J. *Acta Crystallogr.* **1976**, *B32*, 186–193. (e) Lock, C. J. L.; Speranzini, R. A.; Turner, G.; Powell, J. *J. Am. Chem. Soc.* **1976**, *98*, 7865–7866. (f) McCall, M. J.; Taylor, M. R. *Biochim. Biophys. Acta* **1975**, *390*, 137–139.

(57) Gagnon, P. C.; Beauchamp, A. L. *Acta Crystallogr.* **1977**, *B33*, 1448–1454.

(58) De Meester, P.; Goodgame, D. M. L.; Skapski, A. C.; Warne, Z. *Biochim. Biophys. Acta* **1973**, *324*, 301–303.

(59) (a) McCall, M. J.; Taylor, M. R. *Biochim. Biophys. Acta* **1975**, *390*, 137–139. (b) Scwarz, F.; Lippert, B.; Schöllhorn, H.; Thewalt, U. *Inorg. Chim. Acta* **1990**, *176*, 113–121. (c) Olivier, M. J.; Beauchamp, A. L. *Inorg. Chem.* **1980**, *19*, 1064–1067.

terms of having simultaneous metal chelation to N3 and N4 of 1-methylcytosine in a four-membered ring. This Pt(IV) complex shares some common structural features with **4** in that the cytosine chelate rings in both complexes are planar and exhibit the same constricted N4–C4–N3 bond angle of 106°.

To date, we are aware of only two other diffraction studies of metallocene–nucleobase complexes. The crystal structure of Cp_2Ti(theophylline)[61] indicates Ti(III) chelation by the N7 and O6 atoms of the theophylline oxopurine. In addition, the crystal structure of $Cp_2Ti(Cl)$(purine)[62] reveals Ti(IV)–N9 coordination. Both structures are proposed to model the coordinative inter- and intrastrand cross-linking of DNA via Cp_2Ti–nucleobase binding. However, such models must be regarded as highly speculative since the complexes are isolated from nonaqueous media (THF), do not take into account the poor hydrolytic stability of the Ti–Cp framework,[12] and do not address the hydrolytic stability of the Ti–N bond in H_2O.

Cp_2Mo^{2+} Coordination to 2′-Deoxymononucleotides. The present studies of Cp_2Mo^{2+} coordination to 2′-deoxynucleotides and to the monomethylphosphate ester of 5′-dGMP serve as models in understanding the interaction of Cp_2MoCl_2(aq) with the basic building blocks of DNA. The NMR spectroscopic and X-ray crystallographic studies show that Cp_2Mo^{2+} coordinates to N7 and O(phosphate) of purine mononucleotides, resulting in monomeric Cp_2Mo(5′-dAMP) and dimeric Cp_2Mo(5′-dGMP) adducts. The analogous complexes with 5′-dCMP and 5′-dTMP likely have similar structures. The Cp_2Mo(5′-dAMP) monomer represents a rare example of a mononuclear metal–nucleotide complex where the metal binds to N7 and O(phosphate) of the same nucleotide. Previous crystallographically characterized examples of N7/O(phosphate) coordination are all polynuclear structures in which the metal ions bind to N7 and O(phosphate) of different nucleotide ligands.[63]

The above structural remarks should be supplemented with the present finding that Cp_2Mo^{2+} exhibits little selectivity in nucleotide binding and that Cp_2Mo(nucleotide) complexes undergo relatively facile nucleotide exchange. Both observations stand in marked contrast to the behavior of cisplatin.[4,7]

The present crystallographic study of [Cp_2Mo(2′-deoxyguanosine-5′-monophosphate)]$_2$ (**5**) is one of the few available investigations of a 2′-deoxyribonucleotide metal complex. The vast majority of structural studies have involved ribonucleotides. Most involve metal–nucleobase and/or phosphate coordination and most are polynuclear.[63] In close similarity to **5**, the complexes [Pt(5′-CMP)(en)]$_2$,[63a] [Cu_3(5′-GMP)$_3(H_2O)_8]_n$,[63c] and [Cd(5′-CMP)$(H_2O)]_n$[63g] also feature a chelation mode involving simultaneous metal coordination to the nucleobase and phosphate moiety of different nucleotides.

The conformation of the 5′-dGMP unit in **5** displays some unusual geometrical distortions. The coordination of Cp_2Mo^{2+} to 5′-dGMP changes the sugar puckering from O4′-endo to C3′-endo and alters the glycosidic conformation from anti to syn. The syn glycosidic conformation in **5** is unusual in that most crystallographic studies of metal–purine nucleotide complexes reveal a C3′-endo/anti combination.[49,63] This present exception may be due to the sterically encumbered Cp ligation as well as the geometrical constraints imposed by dimer formation (the NOE data suggest that monomeric **6** has an anti conformation). A nucleotide distortion similar to that in **5** has been noted in the crystal structure of (2,2′-bipyridine)copper(II) uridine-5′-monophosphate,[64] which shows an unusual C3′-endo and O1′-endo sugar puckering, and the rare syn glycosidic conformation.

In regard to the phosphate coordination in **5**, the 33 ppm downfield shift in the ^{31}P NMR signal (observed in solution and the solid state) relative to free Na_2(5′-dGMP) is unusually large. While ^{31}P chemical shift displacements of this magnitude are usually associated with major distortions of the phosphorous valence geometry,[35] distortions of this magnitude are not found in the crystal structure of **5**. In addition, direct phosphate coordination to Pt and other diamagnetic metal centers seldom effects a ^{31}P chemical shift displacement greater than 5 ppm.[65]

Implications for Cp_2Mo^{2+} Coordination to Polynucleotides. In the case of cisplatin, there is now compelling evidence that the key antineoplastic metal–DNA interaction involves relatively nonlabile intrastrand chelation of $(NH_3)_2Pt^{2+}$ by the N7 sites of two proximate guanosine residues.[4,7] In regard to structural/mechanistic parallels in Cp_2MX_2–DNA chemistry, the present results and the bulk of other evidence argue that the interaction cannot be similar. Thus, while recent studies have identified aqueous DNA binding (of unknown structural characteristics) by Cp_2MCl_2(aq), where M = Ti, Zr, Hf, and Nb,[66] it is noteworthy that the M = Zr and Hf complexes are reported to have negligible antitumor activity.[1,2] Furthermore, these same binding studies detected no DNA binding in the case of antineoplastic Cp_2VCl_2.[66]

The present results with Cp_2MoCl_2 provide the first detailed metrical information on the types of metallocene coordinative interactions that are possible with DNA constituents. Particularly noteworthy is the importance of phosphomonoester Mo–O binding, the relative unimportance of Mo–O phosphodiester binding, and the formation of chelates with nucleobases as well as the nonselectivity and relative lability of Cp_2Mo^{2+}–nucleotide binding. The present results also underscore the greatly different steric constraints imposed upon DNA coordination by $(NH_3)_2Pt^{2+}$ and Cp_2Mo^{2+} ancillary ligation. In the former case, many types of sterically encumbered ligands can be readily accommodated in the plane(s) perpendicular to the molecular square plane, such as N7 coordination by two mutually tipped (noncoplanar) guanosine residues.[7] In contrast, the steric constraints imposed by the Cp ligands render such arrangements energetically unfavorable in Cp_2M^{2+} coordination spheres, and most bulky planar ligands are typically accommodated in the equatorial girdle (e.g., Cp_2Mo(pyrazolate)$_2$,[26d] **13** vs **14**).

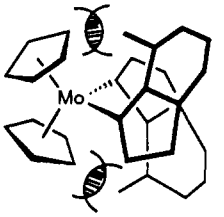

13

14

With reference to parallels between $(NH_3)_2Pt^{2+}$–DNA and Cp_2Mo^{2+}–DNA binding, attempts were made using molecular graphics techniques, to dock a Cp_2Mo^{2+} moiety via N7 coordination to a chelating d(pGpG) portion of an energy-minimized d(ApGpGpT)/d(TpCpCpA) duplex (see Experimental Section for additional details). Cp_2Mo–N metrical parameters were taken from the present crystallographic data. It is found that severe nonbonded interactions are encountered in the major groove be-

(60) (a) Schöllhorn, H.; Beyerle-Pfnur, R.; Thewalt, U.; Lippert, B. *J. Am. Chem. Soc.* **1986**, *108*, 3680–3688. (b) Beyerle-Pfnur, R.; Schöllhorn, H.; Thewalt, U.; Lippert, B. *J. Chem. Soc., Chem. Commun.* **1985**, 1510–1511.

(61) Cozak, D.; Mardhy, A.; Olivier, M. J.; Beauchamp, A. L. *Inorg. Chem.* **1986**, *25*, 2600–2606.

(62) Beauchamp, A. L.; Cozak, D.; Mardhy, A. *Inorg. Chim. Acta* **1984**, *92*, 191–197.

(63) (a) Bau, R.; Gellert, R.; Lehouse, S. M.; Louie, S. *Wadley Med. Bull.* **1977**, *7*, 51–62. (b) Aoki, K. *Acta Crystallogr. B* **1976**, *22*, 1454–1460. (c) Aoki, K.; Clark, G. R.; Orbell, J. D. *Biochim. Biophys. Acta* **1976**, *425*, 369–371. (d) Goodgame, P.; Jeeves, I.; Phillips, F. L.; Skapski, A. C. *Biochim. Biophys. Acta* **1975**, *378*, 153–157. (e) Gellert, R. W.; Bau, R. *J. Am. Chem. Soc.* **1975**, *97*, 7379–7380. (f) Aoki, K. *Bull. Chem. Soc. Jpn.* **1975**, *48*, 1260–1271. (g) Clark, G.; Orbell, J. D. *J. Chem. Soc.* **1975**, 697–698. (h) deMeester, P.; Goodgame, D. M. L.; Jones, T. J.; Skapski, A. C. *Biochim. Biophys. Acta* **1974**, *353*, 392–394.

(64) Fisher, B. D.; Bau, R. *Inorg. Chem.* **1978**, *17*, 27–37.

(65) (a) Marzilli, L. G.; Kline, T. P.; Live, D.; Zon, G. *ACS Symp. Ser.* **1989**, *402*, 119–145. (b) Geraldes, C. F. G. C.; Castro, M. M. C. A. *J. Inorg. Biochem.* **1986**, *28*, 319–327. (c) Marzilli, L. G.; Reily, M. D.; Heyl, B. L.; McMurray, C. T.; Wilson, W. D. *FEBS* **1984**, *176*, 389–392. (d) den Hartog, J. H.; Altona, C.; van Boom, J.; Reedijk, J. **1984**, *176*, 393–397. (e) Cohn, M.; Hughes, T. R. *J. Biol. Chem.* **1962**, *237*, 176–181.

(66) McLaughlin, M. L.; Cronan, J. M., Jr.; Schaller, T. R.; Snelling, R. D. *J. Am. Chem. Soc.* **1990**, *112*, 8949–8952.

tween the Cp ligands and the two guanosine residues as well as between the Cp ligands and the phosphate backbone (Figure 18). The modeling studies show that Cp_2Mo^{2+}–nucleobase bidentate coordination to mutually tipped guanosine residues such as those in *cis*-$[Pt(NH_3)_2\{d(pGpG)\}]$[7a,d] is also sterically impaired. These observations are in agreement with results to be reported elsewhere[67] which indicate that the binding of $Cp_2VCl_2(aq)$ or $Cp_2MoCl_2(aq)$ to DNA plasmids and the subsequent effects on DNA processing enzymes are greatly different from those of cisplatin.[4,7] While NMR data provide no evidence for strong $Cp_2MoCl_2(aq)$ binding to various ribose/nucleobase-terminated model oligonucleotides, binding is observed to 5′-phosphate terminated oligonucleotides.[67] Thus, it is likely that the mechanism(s) of Cp_2MX_2 antineoplastic activity is (are) quite different from that (those) of cisplatin. It if furthermore conceivable that mechanisms are different for different metallocene drugs, and these possibilities are presently under investigation.

(67) (a) Liu, A. H.; Kuo, L. Y.; Marks, T. J., manuscript in preparation. (b) Liu, A. H.; Marks, T. J., manuscript in preparation.

Acknowledgment. This research was supported by NSF (Grant CHE8800813). L.Y.K. was a Dee and Moody Predoctoral Fellow. We thank Dr. W. C. Finch for assistance with the solid-state ^{31}P NMR spectroscopy and Dr. A. H. Liu for assistance with the molecular graphics.

Supplementary Material Available: Tables of atomic coordinates (Tables III, IV, and IX) and anisotropic thermal parameters for **3a**, **4**, and **5**, hydrogen atom positions for **3a** and **4**, and ^1H–^1H coupling constants and derived conformational populations for **5**, **6**, and **7a** (10 pages); listings of observed and calculated structure factors from the final cycles of least-squares refinement for **3a**, **4**, and **5** (78 pages). Ordering information is given on any current masthead page.

Ab Initio Prediction of the Structures and Stabilities of the Hyperaluminum Molecules: Al_3O and Square-Planar Al_4O

Alexander I. Boldyrev[†] and Paul von R. Schleyer*

Contribution from the Institut für Organische Chemie, Friedrich-Alexander Universität Erlangen-Nürnberg, Henkestrasse 42, D-8520 Erlangen, Germany. *Received February 4, 1991*

Abstract: The concept of hypermetalation, characterized by molecules with unprecedented stoichiometries, is extended to the aluminum–oxygen combinations, Al_3O and Al_4O. Their equilibrium geometries and fundamental frequencies, as well as those of the isolated reference species AlO, Al_2, Al_2^+, Al_2O, Al_3O^+, Al_3O, Al_3^+, Al_4^{2+}, and Al_4O, were calculated at HF/6-31G* and at various correlated levels, e.g., MP2(full)/6-31G*. Extensive searches of possible structures and electronic states were carried out. The global minima are: linear Al_2O ($D_{\infty h}$, $^1\Sigma_g^+$), planar Al_3O^+ (D_{3h}, $^1A_1'$), planar Al_3O (the C_{2v} $Y(^2A_1)$ and $T(^2B_2)$ forms have nearly the same energy), tetrahedral Al_4^{2+} (T_d, $^1A_1$), and planar Al_4O (D_{4h}, $^1A_{1g}$). All these species are very stable (with the exception of Al_4^{2+}) with regard to all possible decomposition pathways. Representative dissociation energies (in kcal/mol at PMP4SDTQ/6-311+G*//MP2(full)/6-31G*+ZPE) are: Al_3O^+, into $Al_2O + Al^+$ (34.1); Al_3O, into Al_2O + Al (19.9); Al_4O, into Al_3O + Al (45.5) or into $Al_2O + Al_2$ (37.1). Although the aluminum–oxygen attraction is largely ionic, aluminum–aluminum bonding contributes significantly to the stability of the hyperaluminum Al_3O and Al_4O molecules.

Introduction

We have discovered a remarkable molecule, Al_4O, computationally. The oxygen is surrounded by four aluminum atoms in a square-planar (D_{4h}) arrangement. The electronic structure, combining ionic and substantial metal–metal bonding, anticipates a large, new class of similar molecules.

Such "hypermetalation" involving alkali metal stoichiometries exceeding normal valence expectations is now well-documented. Many of hyperlithium molecules (OLi_4, OLi_5, OLi_6, NLi_5, CLi_5, CLi_6, BLi_5, $BeLi_4$, $BeLi_6$, Cs_4O, etc.) were discovered computationally.[1-11] Li_3O, Li_4O, and Li_5O have been observed mass spectrometrically and the atomization energies determined.[12,13] There is similar evidence for Na_2Cl,[14] Na_3O, Na_4O, K_3O, K_4O,[15,16] and Cs_8O.[17] The "suboxides" of rubidium and cesium, e.g., Rb_9O_2, Cs_7O, and $Cs_{11}O_3$, have been characterized.[18,19] The substantial stability of these molecules is due to the high degree of ionic character as well as bonding interactions between the ligand atoms.[1-7] In a sense, hypermetalated species can be regarded as metal clusters bound ionically to a centrally located "impurity" heteroatom. This contrasts with the usual situation in which the only bonding interactions are between the central atom and its attached atoms or ligands, e.g., in methane, where the ligand–ligand interactions are repulsive. Hence, the usual valence theory, which does not include all the possible interatomic interactions as bonding possibilities, must be modified.

[†] Permanent address: Institute of Chemical Physics, USSR Academy of Sciences, Moscow V-334, Kosygin str. 4, USSR.

(1) Schleyer, P. v. R.; Wurthwein, E.-U.; Pople, J. A. *J. Am. Chem. Soc.* **1982**, *104*, 5839.
(2) Schleyer, P. v. R. *New Horizons of Quantum Chemistry*; Lowdin, P.-O., Pulman, A., Eds.; Reidel: Dordrecht, 1983; pp 95–105.
(3) Schleyer, P. v. R.; Wurthwein, E.-U.; Kaufmann, E.; Clark, T. *J. Am. Chem. Soc.* **1983**, *105*, 5930.
(4) Schleyer, P. v. R.; Tidor, B.; Jemmis, E. D.; Chandrasekhar, J.; Wurthwein, E.-U.; Kos, A. J.; Luke, B. T.; Pople, J. A. *J. Am. Chem. Soc.* **1983**, *105*, 484.
(5) Schleyer, P. v. R. *Pure Appl. Chem.* **1984**, *56*, 151.
(6) Schleyer, P. v. R.; Reed, A. E. *J. Am. Chem. Soc.* **1988**, *110*, 4453.
(7) Reed, A. E.; Schleyer, P. v. R.; Janoschek, R. *J. Am. Chem. Soc.* **1991**, *113*, 1885.
(8) Pewestorf, W.; Bonacic-Koutecky, V.; Koutecky, J. *J. Chem. Phys.* **1988**, *89*, 5794.
(9) Fantucci, P.; Bonacic-Koutecky, V.; Pewestorf, W.; Koutecky, J. *J. Chem. Phys.* **1989**, *91*, 4229.
(10) Klimenko, N. M.; Musaev, D. G.; Gorbik, A. A.; Zyubin, A. S.; Charkin, O. P.; Wurthwein, E.-U.; Schleyer, P. v. R. *Koord. Khim.* **1986**, *12*, 601.
(11) Savin, A.; Preuss, H.; Stoll, H. *Rev. Roum. Chim.* **1987**, *32*, 1069.
(12) Wu, C. H. *J. Chem. Phys.* **1976**, *65*, 3181.
(13) Wu, C. H. *Chem. Phys. Lett.* **1987**, *139*, 357.
(14) Peterson, K. I.; Dao, P. D.; Castleman, A. W., Jr. *J. Chem. Phys.* **1983**, *79*, 777.
(15) Dao, P. D.; Peterson, K. I.; Castleman, A. W., Jr. *J. Chem. Phys.* **1984**, *80*, 563.

0002-7863/91/1513-9045$02.50/0